Cluster analysis of multiparticle final states for medium-energy reactions

H. Schiller

Institute of High Energy Physics, GDR Academy of Sciences, Berlin
Fiz. Elem. Chastits At. Yadra **11**, 182–235 (January–February 1980)

It is difficult to study hadron interactions with several final particles because of the high dimensionality of the phase space. The dynamical mechanisms of one final state produce a structure of the density distribution in the phase space. This structure can be studied by cluster analysis with minimal *a priori* knowledge. A cluster algorithm is proposed that takes into account the orientation and shape of a cluster. Application of this algorithm to the reactions $\pi^{\pm}p \to p\pi^{\pm}\pi^{+}\pi^{-}$ ($p_{\text{lab}} = 16$ GeV/c) and $K^{-}p \to pK^{0}\pi^{0}\pi^{-}$ ($p_{\text{lab}} = 10$ GeV/c) reveals the dynamical mechanisms with small cross section. The applicability of the methods is discussed.

PACS numbers: 13.85.Hd, 12.40.Ss, 11.80.Cr

"It can only be regretted that some people are still satisfied with an analysis of data at a superficial level, which guarantees in advance the absence of new results." Ludwig Van Hove

INTRODUCTION

The experimental and theoretical study of multiparticle production processes is one of the most important tasks of high energy physics. With increasing multiplicity, the elucidation of the particle production mechanicms by means of one- and two-dimensional projections of the phase space becomes more and more complicated. The exclusive analysis of multiparticle reactions has been developed in two independent directions:

1. Variations are sought that describe one definite property of an entire reaction; these variables use information about all the produced particles. They can be called collective variables, since they characterize the event as a whole (with all final particles).[1-7]

2. An attempt is made at the complete analysis of the kinematic information of one reaction channel[8,9] and at the separation (and description) of all processes.

Experimental and theoretical investigations of multiparticle production are becoming more important, since on the transition to higher energies and electronic experiments[10] the experimental information on reactions with high multiplicity rapidly increases.

The study of reactions with several final particles showed that processes in which low-mass resonances are produced make a large contribution to the cross section.[11] As the multiplicity increases, so does the difficulty in identifying the as yet unknown mechanisms of production of a given final state and disentangling them. Because of kinematic reflections and overlapping with other reactions, simple distributions with respect to the effective mass frequently do not permit any conclusions to be drawn.[12]

On the basis of one-dimensional distributions, one can study the density distribution in space produced by the complete set of independent kinematic variables.

For an n-particle final state, the number of independent variables at a definite energy and for unpolarized particles is large ($3n-5$), which makes a complete analysis difficult.

An important step in this direction is an investigation with respect to the longitudinal momentum.[13] It is based on the experimentally observed fact that the mean transverse momentum of the produced particles depends effectively on neither the energy, nor the multiplicity, nor the particle species. It is therefore expected that the longitudinal momenta contain the decisive dynamical information.

However, an analysis with respect to the longitudinal momentum of a final state, in particular with four particles, permits separation into only four groups. One achieves physical separation into diffraction of a nucleon and a meson and into meson exchange reactions. The different states of meson diffraction, for example, are not separated.

It is difficult to apply longitudinal-momentum analysis for final states with five or six particles[14,15] at medium energies, since here numerous mechanisms do not occur in one sector of the diagram of the longitudinal phase space.

A prism-plot analysis[8] was used in a first attempt to investigate simultaneously all the mechanisms belonging to one final state in a $(3n-5)$-dimensional phase space. The basic idea is as follows: The experimentally observed density distribution is approximated by the density distribution of events obtained by the Monte Carlo method in accordance with a given list of reaction mechanisms. As a result of iterations, one obtains the distribution of the experimental events due to the considered reaction mechanisms together with their relative contributions.

The prism-plot analysis uses complete kinematic information. However, it has a shortcoming, in that it requires a more or less detailed knowledge of the investigated channel.

Each event of the reaction

$$a+b \to 1+2+\ldots+n$$

 0090-4759/80/010071-20$02.80 © 1980 American Institute of Physics

at constant energy and for unpolarized particles of the initial state can be uniquely described by $3n-5$ independent kinematic variables x. The events of the investigated reaction are distributed in the space of the kinematic variables within a region with boundary defined by energy and momentum conservation. Within this region, the density distribution of the points (events) is

$$d\sigma/dx = k(x) \mid T(x) \mid^2,$$

where $k(x)$ is a kinematic factor that depends on the choice of the variables x, and $T(x)$ is the transition matrix element of the given reaction.

In general, the final state contains some subprocesses z:

$$\frac{1}{k(x)}\frac{d\sigma}{dx} = \mid T(x) \mid^2 = \Big| \sum_{z=1}^{Z} T_z(x) \Big|^2.$$

Ignoring the interference terms, we obtain

$$\frac{1}{k(x)}\frac{d\sigma}{dx} = \sum_{z=1}^{Z} \mid T_z(x) \mid^2.$$

In this (ideal) case, the points representing the events of each of the participating subprocesses produce one or several (almost nonoverlapping) maxima of the density. At medium energies, this ideal case is not encountered, since at such energies overlappings and the interference terms are important. Nevertheless, analysis of the $(3n-5)$-dimensional distribution of the points is of interest, since in many cases the overlappings are small,[16] and as a result of the interference there may arise additional maxima of the density and subprocesses of small cross section can sometimes be found only after separation of a subprocess of large cross section.

In the literature, a maximum of the density of the points representing the events in the multidimensional phase space is called a cluster.

It is proposed to study the $(3n-5)$-dimensional distribution of the points by methods developed in other fields (in psychology, biology, and pattern recognition) for cluster analysis.

Of particular interest are methods based on knowledge of the basic structure of the maxima of the points but which do not require further assumptions about $T_z(x)$.

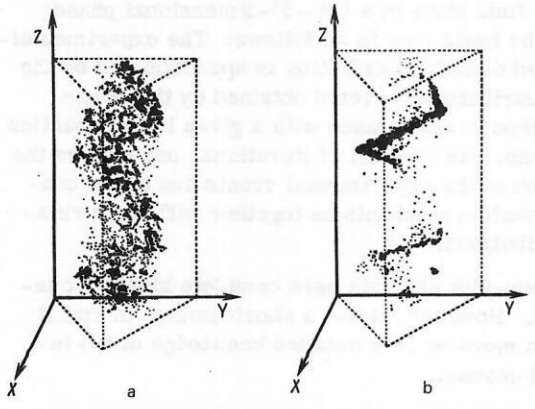

FIG. 1. Prism plot for Monte Carlo generated events (invariant phase space) (a) and for experimental data (b). The reaction is $\pi^+p \to p\pi^+p\pi^0$ at $p_{lab} = 3.9$ GeV/c.

A cluster found in this manner is obviously not a consequence of the original assumptions but is automatically obtained from the structure of the distribution of the points in the $(3n-5)$-dimensional space.

A prerequisite of such cluster analysis is the experimental fact that the events are concentrated in relatively small regions of phase space (Fig. 1). The maxima of $|T_z|^2$ are narrow compared with the kinematically allowed phase space, so that the distribution of the points in the phase space has a well-defined structure. The existence of such clusters in phase space is revealed by different methods in a wide range of energies and for a set of reactions.[14,17-21]

1. METHODS OF CLUSTER ANALYSIS

Cluster analysis is used to solve numerous problems. Generally spaaking, the aim of cluster analysis is to divide data into groups such that the elements of one group are similar to each other, while different groups are not similar. The main difficulty in cluster analysis is that the expressions "similar" and "not similar" acquire meaning only when applied to a definite problem.[22] The problem of analyzing concentrations of points in spaces of high dimensionality is encountered, for example, in technology (pattern recognition), in sociology and psychology (the finding of structures in a given population—questionnaires and surveys), in medicine (automatic diagnosis of general examinations), etc. There are proposed and used as many algorithms for finding clusters as there are applications for such analysis. In the absence of a general definition of a cluster, one can discuss the efficiency of a cluster algorithm only in connection with its use. The algorithms differ considerably in the size of the programs and depend on the capabilities of the computational techniques.

We present here a systematization of the existing cluster algorithms in connection with their use in high energy physics.

Hierarchical Methods. The epithet "hierarchical" means that the objects (events) are regarded as the end points of the branches of a "tree," and the nodes of one level correspond to one set. A higher level corresponds to a more general set.

1. Classification in accordance with a similarity matrix (or distance matrix). When there are N points, this matrix contains $N(N-1)/2$ elements, so that it may be difficult to use it for a large number of points.

2. Graphical minimum spanning tree (MST) method. The N points are regarded as the nodes of a connecting graph, i.e., the graph has $N-1$ connections, so that any pair of connections corresponds uniquely to one link segment. With the links are associated the distance to the point of the corresponding node. One then constructs a connecting graph corresponding to the minimal sum of distances (MST). The graph is divided with respect to the longest span. The resulting subgraphs are divided in the same way, and in this way a hierarchy of clusters is obtained.[23]

Application of this algorithm to 1000 events of the re-

action $\pi^+p \to p\pi^+\pi^0$ at $p_{1ab}=5$ GeV/c led to the following conclusions[24]: the minimum spanning tree has in regions of overlapping of the concentrations links which are shorter than in the neighboring regions (therefore, the method described above does not give a physical correspondence of the events with a dynamical mechanism); the maximal link in the minimum spanning tree described in Ref. 23 can, as a method of rough description of structure in an analysis of data, serve to divide the concentrations shown in Fig. 1.

3. Hierarchy of possible clusters by an estimate for each event of the density of the surrounding points. After the events have been ordered in accordance with decreasing density of the points, the following procedure is carried out.

Event 1 determines the center of the first cluster. To this cluster one adds events whose density is greater by the factor λ than the density of the first point and whose distances to event 1 are not greater than νR, where R is the mean distance of the neighbors k and $k+1$ from event 1 (ν is a parameter of the algorithm).

The first event that satisfies the first but not the second condition determines the center of cluster 2, etc. The results of the analysis depend strongly on the values of the parameters ν and λ. Large λ permit one to study only clusters of high density that are well separated and do not depend on the choice of ν. Choosing λ to be smaller and smaller, one can combine neighboring clusters. Large values of ν facilitate the combination of clusters.

The application of this method to the reactions $K^-p \to p\bar{K}^0\pi^-$ and $K^-p \to K^-\pi^+n$ at $p_{1ab}=4.2$ GeV/c is described in Ref. 25. This analysis did not use the density of points in phase space but estimated the square of the matrix element

$$|T(x)|^2 \sim (1/J^x)\Delta N/\Delta V,$$

where J^x is the density of the phase space at the point x. The variables x used were the Van Hove angle ω, $p_t^2(n)$, $p_t^2(K^-)$, and the angle φ between $\mathbf{p}_t(n)$ and $\mathbf{p}_t(K^-)$, so that

$$\frac{1}{J^x}=\left[\sum_{j=1}^{3}\frac{p_{t,j}^{*2}}{E_j^*}\right]\left[\sum_{j=1}^{3}p_{t,j}^{*2}\right]^{-1}\left[\prod_{j=1}^{3}E_j^*\right].$$

In estimating $\Delta N/\Delta V$, we choose K nearest neighbors ($K\sim 30$), and we calculate ΔV from $\Delta V=R^{3n-5}$, where R is the mean distance from the point for which we estimate the density to neighbors k and $k+1$. For the reaction $K^-p \to pK^0\pi^-$, there were found, besides the dominant clusters $K^*(890)$ and $K^*(1420)$, the cluster $Y^* \to \bar{K}^0p$ and others with $\Delta^0(1236)$, $N^{*0}(1470)$, and $N^{*0}(1700)$. Some of the remaining groups with ≤ 10 points (events) had superhigh transverse momenta.

Analysis of 1500 events of the reaction $K^-p \to nK^-\pi^+$ gave for $\lambda=0.05$ and $\nu=0.53$ three clusters. Cluster 2 contained essentially pure production of $K^*(890)$. For cluster 3, a simple physical interpretation was not found. Cluster 1 is a mixture of $K^*(890)$, $K^*(1420)$, $\Delta^+(1236)$, and the $n\pi^+$ diffraction system. A reduction of the parameter ν to $\nu=0.52$ did not change clusters 2 and 3, but split cluster 1 into four groups: $\Delta^+(1236)$: $\Delta^+(1236)+K^*(1420)$; $\Delta^+(1236)+K^*(890)$; and $K^*(890)+K^*(1420)+$the $n\pi^+$ diffraction system.

The use of such analysis for 1291 events of the reaction $K^-p \to K^-\pi^+\pi^-p$ and 880 events of the reaction $K^-p \to K^-\pi^+\pi^-\pi^0p$ at $p_{1ab}=12.6$ GeV/c is described in Ref. 26, in which it is concluded that the decomposition into clusters reflects the essential properties of the observed reaction mechanisms.

Nonhierarchical Methods. These methods enable one to divide events into clusters without determining their hierarchical structure.

1. Method of centers. The N points X_i are divided into K groups. The center of each group is determined. A new subdivision is obtained in such a way that each point is joined to the group whose center is nearest. In general, this procedure leads very rapidly to convergence. Some initial groups may "die out." This method is used in the algorithm given in Appendix 1.

If the second moments are taken into account in this method, the algorithm CLUCOV (see below) is obtained.

An expansion of the density of the points with respect to orthogonal functions and study of the obtained analytic expression are very difficult because one does not know the order at which the expansion must be terminated, and because of the large number of terms that must be taken into account.

2. Iterative cluster analysis. Developed at CERN,[27] the method is as follows. Suppose the density of the points (the distribution of the probability density of the points X) is a mixture of K distributions:

$$f(X \mid b^*)=\sum_{k=1}^{K}c_k f_k(X \mid b_k^*).$$

Here, b_k^* are parameters that characterize distribution k.

The problem of cluster analysis is to find an estimate b of the quantities b^* in accordance with the observed distribution of points. One can show that, by finding the maximum of the mean logarithm of the likelihood,

$$\eta(b \mid b^*)=E\{\ln f(X \mid b)\}=\int \ln[f(X \mid b)]\, f(X \mid b^*)\, dx,$$

one obtains an estimate of the maximal likelihood parameter of the given distribution.

If $f(X \mid b^*)$ is a superposition of K nonoverlapping Gaussian functions with weights c_k and covariations Σ_k, this method requires the finding of the maximum of the function

$$\eta_G(b)=\sum_{k=1}^{K}c_k \ln\left\{\frac{c_k}{(\det \Sigma_k)^{1/2}}\right\}.$$

The program developed at CERN enables one to implement an iterative procedure for determining the maximum of the function $\eta_G(b)$ by means of a display.[28-31]

An important property of this procedure is the constant number K of groups.

3. The method of nonlinear projection $Y=f(x)$ of points x from the multidimen-

sional space onto the two-dimensional plane Y. This method can be used for cluster analysis if the projection $f(x)$ is such that the distance between points is changed little:

$$\sum_{i=2}^{N}\sum_{j=1}^{i}\{\rho_x(x_i x_j)-\rho_y(f(x_i)f(x_j))\}^2.$$

Besides the almost arbitrary choice of the projection f, this method has one further serious shortcoming in that it ignores the shapes of the concentrations of points. At CERN, it was applied to bubble-chamber data.[32]

4. Valley finding method. It is described in detail in Ref. 33.

First Applications of Cluster Analysis in High Energy Physics. In 1972, cluster analysis was applied for the first time to data obtained in bubble chambers. Factor analysis[34] and a method of finding the maximal density similar to that proposed in Ref. 25 were used. Both methods were applied to the reaction $\pi^-p\to p\pi^+\pi^-\pi^-$ at beam momentum 16 GeV/c.[16] The first results confirmed the general correctness of the ideas. However, application to a large body of data led to considerable technical difficulties. A simpler algorithm was required. The valley finding algorithm[34] was chosen.

This method was used to investigate the reactions

$$\pi^+p\to p\pi^+\pi^+\pi^- \quad \text{at 8 GeV/}c, \tag{1}$$
$$\pi^+p\to p\pi^+\pi^+\pi^- \quad \text{at 16 GeV/}c, \tag{2}$$
$$\pi^+p\to p3\pi^+2\pi^- \quad \text{at 16 GeV/}c. \tag{3}$$

The results are considered below.

1. The reaction $\pi^+p\to p\pi^+\pi^+\pi^-$ at 8 GeV/c.[35] The valley finding algorithm was applied to 4400 events of the reaction (1). In general, the kinematic variables for describing one event can be freely chosen. (Some problems in the choice of the variables are considered in Appendix 1.) To investigate the reaction (1), the following variables were chosen:

$$M(p\pi_f^+),\ M(p\pi_s^+),\ M(p\pi^-),\ M(\pi_f^+\pi^-),\ M(\pi_s^+\pi^-); \tag{4}$$
$$M^2(p\pi_f^+),\ M^2(p\pi_s^+),\ M^2(p\pi^-),\ M^2(\pi_f^+\pi^-),$$
$$M^2(\pi_s^+\pi^-),\ t(p/p),\ t(\pi^+/\pi^-), \tag{5}$$

where M is the invariant mass between the particles given in the brackets, t is the four-momentum transfer between the particles, and f and s are the π^+ meson with larger and smaller longitudinal momentum, respectively. The choice of the variables (4) is based on the dominant role of the resonance production mechanism in the reaction.[36] The set of variables (5) is complete; from it one can obtain other sets of independent variables (formed from the squares of the masses and the four-momentum transfers) by linear transformation. Since the cluster structure is not changed after linear transformation, the set (5) is useful for our purposes.

It was found that the results obtained with the choice (5) of the variables were not better than the results obtained with the choice (4). This can be explained as follows: The four-momentum transfers contain little additional information about the clusters; the small number of statistical data (4400 events) does not enable one to exploit fully the method when there is a large number of variables and, thus, separate the clusters better.

TABLE I. Distribution of events over ten clusters in the reaction $\pi^+p\to p\pi^+\pi^+\pi^-$ at 8 GeV/c (4400 events).

Cluster	1	2	3	4	5	6	7	8	9	10
Events	1355	879	651	188	246	232	255	330	76	168

The results presented below were obtained for the set of variables (4) and parameter $R=0.455$ GeV of the valley finding algorithm. Proceeding from 15 initial groups, we obtained ten clusters, and 19 events remained outside groups. The numbers of events in the clusters are given in Table I. In Table II, for each cluster, we give the resonances from which signals are observed in the clusters.

The following conclusions can be drawn: Clusters of events in phase space exist; the clusters obtained frequently by the statistical method correspond to dynamical mechanisms; there are clusters that have several production mechanisms; for some production mechanisms, the method gives good separation of the clusters; the method can be used for a large number of final states.

The cross section of the process $\pi^+p\to\Delta^{++}p^0$ is 406 $\pm$ 28 μb, in good agreement with the results obtained by other methods.[36] The division of this reaction into two clusters is explained by the peripheral nature of the ρ-meson production.

The meson diffraction is separated cleanly, but for the nucleon diffraction a strong overlapping with the subprocess $\pi^+p\to\Delta^{++}f$ is observed. The circumstance that two or more clusters can be obtained as a result of a single production mechanism or that the same cluster can be obtained by several production mechanisms may, at the first glance, appear to be a shortcoming.[12] However, the splitting of one production mechanism into several clusters may also have an important advantage for the analytic description of the mechanism, since it indicates the possible existence of a region where the amplitude vanishes. The impossibility of separating the particle production mechanisms is of particular interest as an indicator of real overlappings in phase space. The production mechanisms not only overlap in the projections (this possibility cannot be eliminated in ordinary analyses) but also in the regions of phase space that contain information on interferences and, thus, on the relative phase of the overlapping mechanisms. In this way, important initial data for multichannel analysis are obtained.[9]

TABLE II. Discovery of resonance signals of ten clusters in the reaction $\pi^+p\to p\pi^+\pi^+\pi^-$ at 8 GeV/c (4400 events).

Cluster	Δ^{++}	Δ^0	ρ_f^0	f_f	ρ_s^0	f_s	N^*_{1470}	N^*_{1700}	A_1	A_2
1	×	—	×	—	—	—	—	—	—	—
2	×	—	×	×	×	×	—	—	—	—
3	×	?	—	×	—	—	×	×	—	—
4	×	—	—	—	—	—	—	?	—	—
5	—	—	×	—	—	—	—	—	×	—
6	—	—	×	—	×	—	—	—	×	×
7	—	—	×	—	×	—	—	—	?	×
8	—	—	×	—	×	—	—	—	—	×
9 and 10	—	—	×	—	×	—	—	—	—	—

TABLE III. Distribution of events over 12 clusters in the reaction $\pi^+p \to p\pi^+\pi^+\pi^-$ at 16 GeV/c (12 529 events).

Cluster	1	2	3	4	5	6	7	8	9	10	11	12
Events	846	2563	395	449	1955	1022	652	1038	1392	66	565	798

Also obtained are two striking clusters (9 and 10) with large longitudinal proton momentum p_f^*. Signals of the ρ and f mesons are obtained in the mass distribution $M(\pi_f^+\pi^-)$. Some of these events can be described by the process $\pi^+_{fl}p \to \Delta(1890)\rho$, which is confirmed by comparison with the same reaction at the momentum $p_{\text{lab}} = 16$ GeV/c.

All the obtained clusters have a remarkable property: They are situated in corresponding regions of the longitudinal phase space. These regions are situated almost within the sectors selected by the longitudinal momentum for separating the corresponding subprocesses.

2. The reaction $\pi^+p \to p\pi^+\pi^+\pi^-$ at 16 GeV/c.[16,37] The valley finding algorithm was applied to 12 529 events of the reaction (2). For comparison, the set of variables (4) was used. Proceeding from 15 initial groups and using the parameter value $R = 0.455$ GeV,[34] we obtained 12 clusters. The populations of these clusters are given in Table III. In Table IV, we give for each cluster the resonances whose signals are observed in the clusters. We shall consider some of these clusters in more detail. To obtain completely the process $\pi^+p \to \Delta^{++}\rho^0$, it is necessary to combine clusters 1–4 (see Table IV and Fig. 2). Study of the distribution of the decay angle of the events of the $\Delta^{++}\rho^0$ process answers the question of why the process is divided into four subprocesses: Each of the obtained clusters contains only one part of the expected distribution of the decay angle, i.e., the dynamics of the process itself forms four clusters in the space of the variables we have employed.

The same can be said of the events that proceed through $\Delta^{++}(1890)\rho$. In cluster 4, there is a clear signal in the region of the $\Delta^{++}(1890)$ mass. The distribution of the decay angle of these events is very asymmetric. Cutting out the region of the $\Delta(1890)$ mass and again combining clusters 1–4, we obtain fairly symmetric distributions of the angles (Fig. 3).

There are also weak signals of the $\Delta^{++}\rho^0$ type in clusters 9, 10, and 12. Together with clusters 6, 7, 8, and 11, these clusters contain basically diffraction dissociation. We ask: Do these processes really overlap in phase space or is the cluster method the origin of these "contaminations"?

TABLE IV. Content of resonance signals of 12 clusters in the reaction $\pi^+p \to p\pi^+\pi^+\pi^-$ at 16 GeV/c (12 529 events).

Cluster	Δ^{++}_{1236}	Δ^{++}_{1890}	ρ^0_f	f^0_f	g^0_f	ρ^0_s	f^0_s	N^*_{1400}	N^*_{1700}	A_1	A_2	A_3	A_4
1	×	—	×	×	×	—	—	—	—	—	—	—	—
2	×	—	×	×	×	—	—	—	—	—	—	—	—
3	×	—	×	×	×	—	—	—	—	—	—	—	—
4	×	×	×	—	—	—	—	—	—	—	—	—	—
5	×	—	—	—	—	—	—	×	×	—	—	—	—
6	—	—	×	×	—	—	—	—	—	×	×	?	×
7	—	—	×	—	—	×	?	—	—	×	?	—	?
8	—	—	×	—	—	×	—	—	—	×	—	—	—
9	?	—	×	×	—	—	—	—	—	?	×	?	—
10	?	—	×	×	—	—	—	—	—	?	×	?	—
11	—	—	×	—	—	×	—	—	—	—	—	×	—
12	?	—	×	—	—	×	—	—	—	—	—	×	—

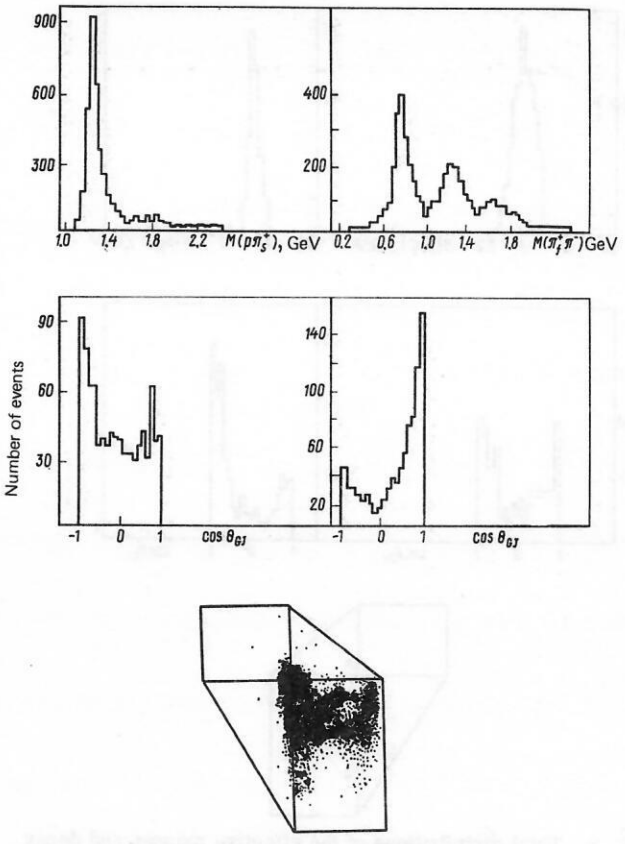

FIG. 2. Total distributions of the effective masses and decay angles and scheme of the longitudinal momenta in the production of the system $\Delta^{++}(1236)\rho^0$ in clusters 1–4 for the reaction $\pi^+p \to p\pi^+\pi^+\pi^-$ at $p_{\text{lab}} = 16$ GeV/c.

Longitudinal-momentum analysis in Ref. 37 led to the suggestion that there is overlapping of the processes $\pi^+p \to pA_3$ and $\pi^+p \to \Delta^{++}\rho^0$, which could be the cause of the observed contaminations. However, in an independent cluster analysis of the reaction (2), a clean separation of these processes was obtained (see Sec. 3). It is therefore necessary to regard the presence of these contaminations (as also in the longitudinal-momentum analysis[37]) as a shortcoming of the method.

Proton diffraction dissociation is contained in a well-separated cluster (Fig. 4). The diffraction spectrum has peaks in the $M(p\pi^+\pi^-)$ mass distribution at 1470, 1700, and 2190 MeV. In the $M(p\pi^+)$ effective-mass distribution one observes the strong Δ^{++} signal typical of this subprocess.

Let us compare the results obtained at 8 and 16 GeV/c. The scheme for separating the mechanisms in the reaction at 8 and 16 GeV/c is shown in Fig. 5. At both energies, overlapping clusters were encountered: One mechanism may participate in the production of different clusters and, conversely, one cluster may be produced by different mechanisms.

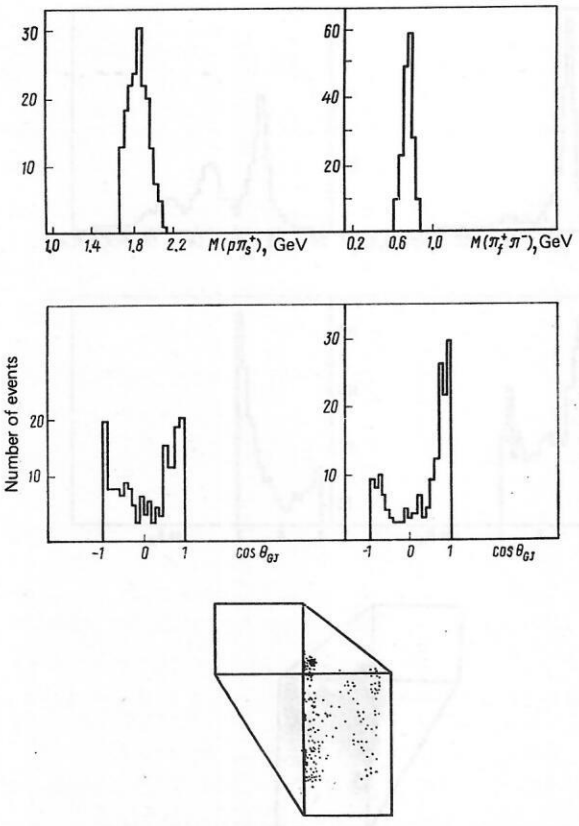

FIG. 3. Total distributions of the effective masses and decay angles and scheme of the longitudinal momenta in the production of the system $\Delta^{++}(1890)\rho^0$ in clusters 1–4 for the reaction $\pi^+p \to p\pi^+\pi^+\pi^-$ at $p_{lab} = 16$ GeV/c; $1.69 \leqslant M(p\pi_s^+) \leqslant 2.09$ GeV, $0.66 \leqslant M(\pi_f^+\pi^-) \leqslant 0.86$ GeV.

Basically, the same clusters are found at 8 and 16 GeV/c. This indicates that the dynamics of the process is the cause of the formation of concentrations in the phase space.

Besides results similar to those obtained at 8 GeV/c, the analysis at 16 GeV/c reveals an appreciable contribution of the process $\pi^+p \to \Delta^{++}(1890)\rho^0$, the presence of the process $\pi^+p \to A_3p$, the possible presence of the process $\pi^+p \to A_4p$, considerably less $N^*\pi/\Delta^{++}f$ overlapping, and the presence of the process $\pi^+p \to \Delta^{++}g$.

The differences concern processes with relatively small cross sections. They can be explained by the higher energy and the greater number of experimental data at 16 GeV/c.

3. The reaction $\pi^+p \to p\pi^+\pi^+\pi^+\pi^-\pi^-$ at 16 GeV/c.[38] The valley finding algorithm was applied to 6317 events of the reaction (3). Two sets of variables were used—the 13 invariant masses

$$M(p\pi_1^+),\ M(p\pi_2^+),\ M(p\pi_3^+),\ M(p\pi_1^-),$$
$$M(p\pi_2^-),\ M(\pi_1^+\pi_2^+),\ M(\pi_1^+\pi_1^-),$$
$$M(\pi_1^+\pi_2^-),\ M(\pi_2^+\pi_1^-),\ M(\pi_2^+\pi_2^-),$$
$$M(\pi_3^+\pi_1^-),\ M(\pi_3^+\pi_2^-),\ M(\pi_1^-\pi_2^-); \quad (6)$$

and the five independent c.m.s. longitudinal momenta:

$$p_L^*(p),\ p_L^*(\pi_1^+),\ p_L^*(\pi_2^+),\ p_L^*(\pi_3^+),\ p_L^*(\pi_1^-). \quad (7)$$

Because of the small number of statistical data, the choice of the variables (4) is preferable. In this analysis too, one subprocess contains different clusters, and vice versa. The subprocesses are not separated so cleanly as in the case of four final particles, but they can provide the point of departure for further investigations. Figures 6–9 show the production of the D meson (Ref. 39), (N^*A_2), $(\Delta^{++}A_2)$, and the double diffraction contribution to the reaction (3).

CLUCOV—a heuristic cluster algorithm.[40] Work with the valley finding algorithm prompted the desire to construct an algorithm with the following properties.[40]

1. The number and position of the maxima of the density must not be known in advance. The algorithm must also be suitable for a variable number of groups. If at some iteration two groups already differ little, they must be combined; if one group has a clear mini-

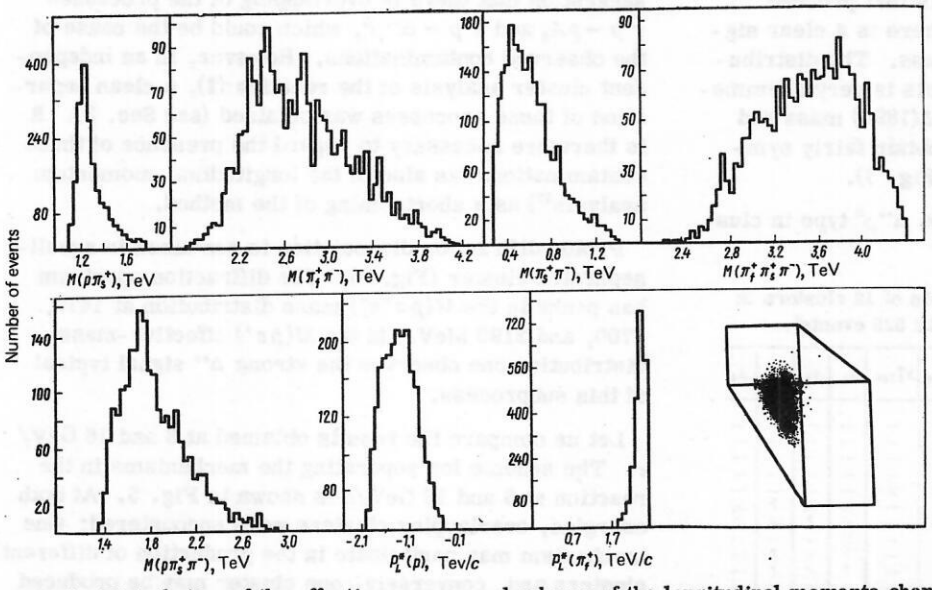

FIG. 4. Distribution of the effective masses and scheme of the longitudinal momenta characterizing diffraction dissociation of the proton for cluster 5 in the reaction $\pi^+p \to p\pi^+\pi^+\pi^-$ at $p_{lab} = 16$ GeV/c (20 168 events).

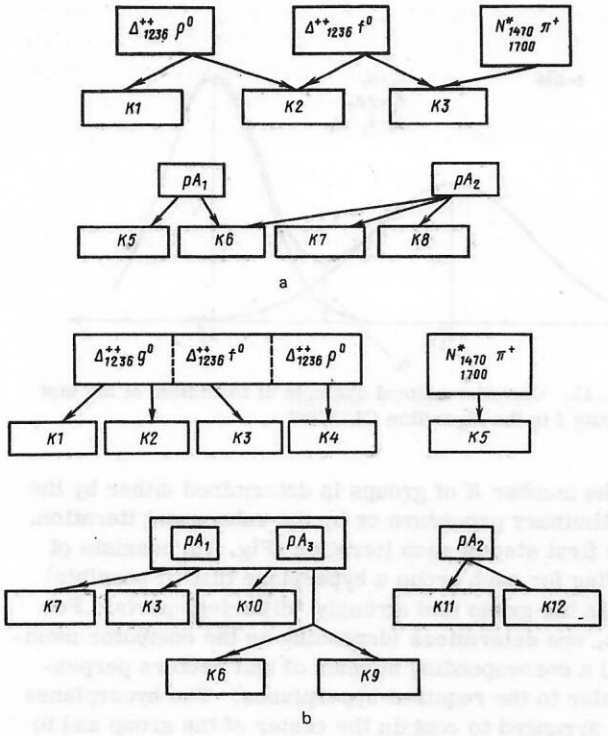

FIG. 5. Scheme of the overlapping of different subprocesses at $p_{1ab} = 8$ GeV/c (a) and at $p_{1ab} = 16$ GeV/c (b). $K1$–$K12$ are clusters.

mum of the density, it must be divided.

2. The algorithm must satisfy the requirement that the found clusters have an ellipsoidal shape of any orientation (see, for example, Fig. 1). This requirement follows from detailed investigations of three-particle final states by means of the usual distributions

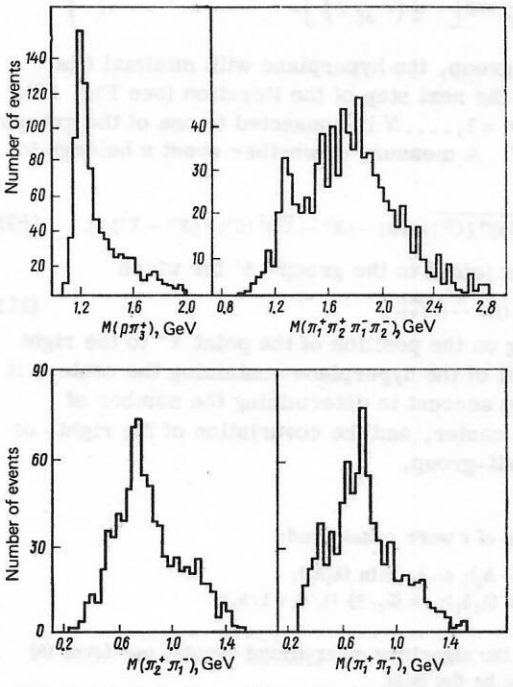

FIG. 6. Distributions of the effective masses characterizing the production of the D meson (cluster 1) for the reaction $\pi^+ p \to p3\pi^+2\pi^-$ at $p_{1ab} = 16$ GeV/c.

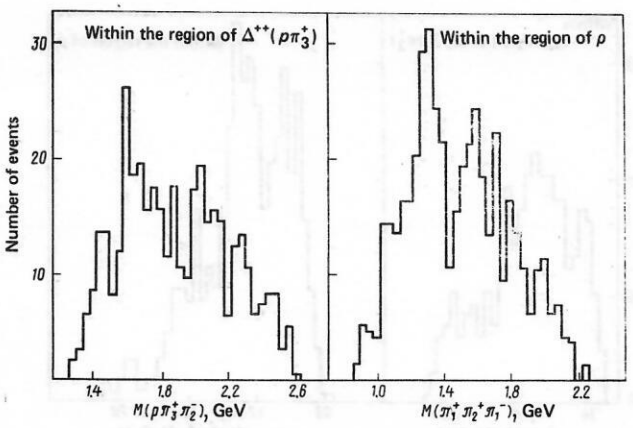

FIG. 7. The same as in Fig. 6 for production of the system N^*A_2 (cluster 14).

(Dalitz plot, prism plot). In addition, it is reasonable to require that two long concentrations of different directions that touch at one end should be divided.

3. The algorithm must analyze channels with 10^4–10^5 events and with 5–18 variables. From this there follow two further technical requirements: The volume of calculations must not increase faster than linearly with the number of events (which rules out algorithms that connect each point to every other); the kinematic information on the events (which is, in general, in an external memory of the computer) must not be used more than once or twice in one iterative step.

The algorithm CLUCOV satisfies these condictions and is a generalization of the method of centers. Here, cluster k is characterized by the moments of zeroth, first, and second order: N^k (content), $\bar{X}^k$ (center), and $C^k_{ij} = (X_i - \bar{X}^k_i)(X_j - \bar{X}^k_j)$ (covariation). To form the moments, the points of group m are used. The program was written in FORTRAN IV and tested on a BESM-6 computer and also on a CDC-7600.

Before the iteration process is carried out, a temporary combining of the points into groups is required. In other words, initial groups are required. For the covariation we take the unit matrix. We obtain the initial centers as follows: A random event determines the first center; we seek the next event with distance great-

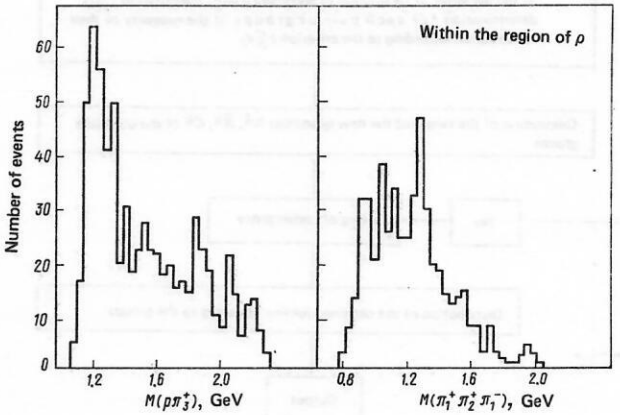

FIG. 8. The same as in Fig. 6 for production of the system $\Delta^{++}A_2$ (cluster 8).

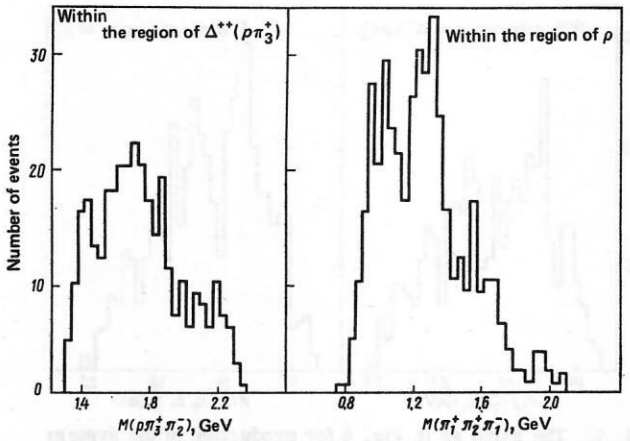

FIG. 9. The same as in Fig. 6 for double diffraction dissociation (cluster 12).

er than the constant R from all the already found centers. If such an event exists, it becomes a center. If it does not, the preliminary procedure has ended.

This procedure has the advantage that all events at a distance less than R are taken with one initial center. It was tested on two-dimensional examples. It was found that the algorithm converges rapidly if two or three times more preliminary groups are created than was assumed for the investigated process.

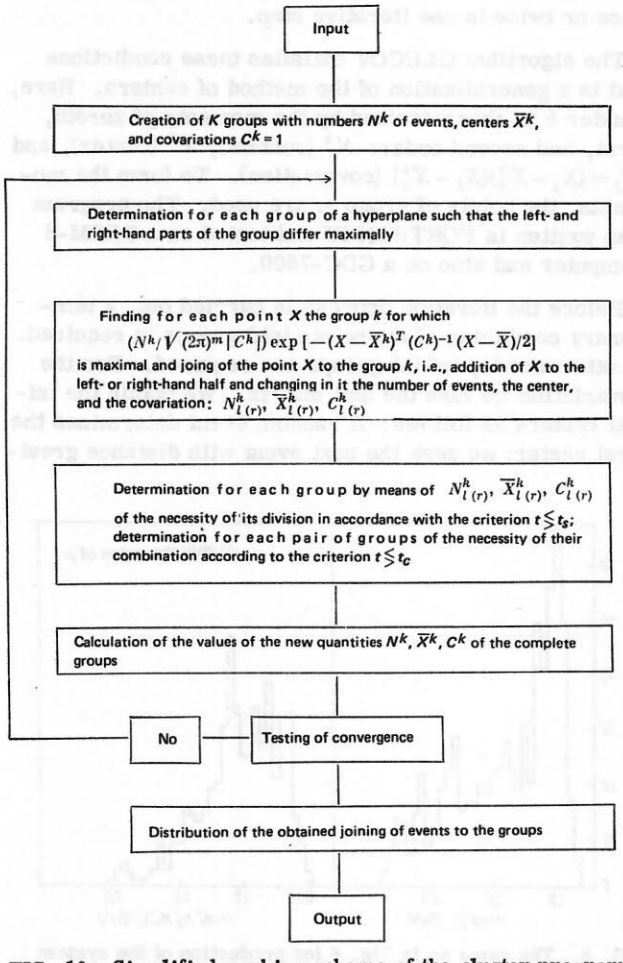

FIG. 10. Simplified working scheme of the cluster program CLUCOV.

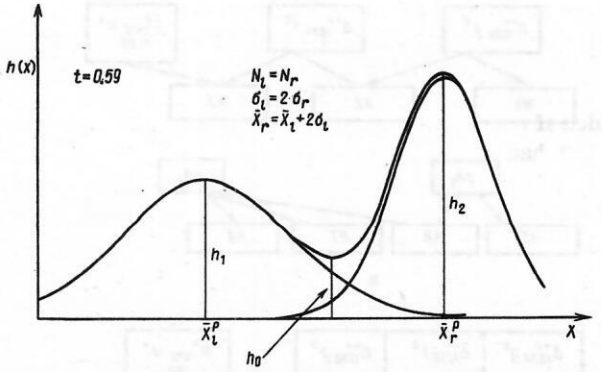

FIG. 11. One-dimensional example of formation of the test quantity t in the algorithm CLUCOV.

The number K of groups is determined either by the preliminary procedure or by the subsequent iteration. The first step of each iteration (Fig. 10) consists of finding for each group a hyperplane that (if possible) splits the group into strongly "differing" parts. For this, one determines (depending on the computer memory) a corresponding number of unit vectors perpendicular to the required hyperplanes. The hyperplanes are arranged to contain the center of the group and to divide the group into left- and right-hand parts, which are projected onto the unit vector normal to the hyperplane. The mean $\overline{X}^p_{l(r)}$ and deviation $\sigma^p_{l(r)}$ of these projections are determined. Then, for each hyperplane the quantity t (Fig. 11) is calculated:

$$t = h_0/\sqrt{h_1 h_2}\ ^{1)}, \tag{8}$$

where

$$\left.\begin{aligned} &h_1 = h(\overline{X}^p_r);\quad h_2 = h(\overline{X}^p_l);\quad h_0 = \min h(X),\quad X \in [\overline{X}^p_l \overline{X}^p_r];\\ &h(X) = \frac{N_r}{\sqrt{2\pi}\,\sigma^p_r} \exp\left[-\frac{1}{2}\left(\frac{X-\overline{X}^p_r}{\sigma^p_r}\right)^2\right] +\\ &+ \frac{N_l}{\sqrt{2\pi}\,\sigma^p_l} \exp\left[-\frac{1}{2}\left(\frac{X-\overline{X}^p_l}{\sigma^p_l}\right)^2\right]. \end{aligned}\right\} \tag{9}$$

For each group, the hyperplane with minimal t is chosen. In the next step of the iteration (see Fig. 10), each event $n = 1, \ldots, N$ is connected to one of the groups $k = 1, \ldots, K$. A measure of whether event n belongs to group k is

$$f^k_n = \left(N^k/\sqrt{(2\pi)^m |C^k|}\right) \exp[-(X^n - \overline{X}^k)^T (C^k)^{-1} (X^n - X^k)/2]. \tag{10}$$

The event is joined to the group[2)] k' for which

$$f^{k'}_n = \max[f^1_n, \ldots, f^K_n]. \tag{11}$$

Depending on the position of the point X^n to the right or to the left of the hyperplane containing the center, it is taken into account in determining the number of events, the center, and the covariation of the right- or left-hand half-group.

[1)] Other forms of t were considered:

$t = 2h_0/(h_1 + h_2)$; $t = h_0/\min(h_1 h_2)$;
$t = h_0/\max(h_1 h_2)$; $t = (h_0/2)(1/h_1 + 1/h_2)$.

In trials of the algorithm on artificial events, our form (8) was found to be the best.

[2)] Some events have a greater separation from all groups than the specified separation. To avoid meaningless deformations of the groups, these events are not joined to any group.

After all points have been joined to the existing groups, the critical value of t is calculated in accordance with (8) for each group. Here, $h(X)$ is the m-dimensional generalization of (9). A group of events is divided if t is smaller than the given t_s, and the right- and left-hand contents, the centers, and the covariations form the characteristics of the new groups in the next iteration. For $t \geq t_s$, the algorithm determines from $N^k_{l(r)}$, $\overline{X}^k_{l(r)}$, $C^k_{l(r)}$ the N^k, X^k, C^k of the complete group for the next iteration. Then it is checked whether there exist pairs of groups with critical value t exceeding the given value t_c. In this case, the groups are regarded as "similar" and the contents, center, and covariation are combined before the following iteration. The iterations are continued as long as the following conditions are fulfilled: a given number of iterations is not exceeded or no group is divided; no groups are combined and the sum of the absolute changes in the contents of the groups is less than a given value.

After convergence has been achieved, the list of events joined to the groups is printed out for further detailed investigations of the clusters. Also printed out is the overlap matrix

$$O_{ik} = \left(\sum_{*} f^k_m \Big/ \sum \sum_{*} f^k_m\right) \cdot 100. \qquad (12)$$

Here, the asterisk denotes the addition of all events m joined to group i.

Figure 12 explains this matrix for the example of three groups shown in the form of Gaussian functions. For each of the three groups, the overlap matrix has the form

$$O = \begin{Bmatrix} (f_1+f_2)/F_1 & f_2/F_1 & 0 \\ f_3/F_2 & (f_3+f_4+f_5)/F_2 & f_5/F_2 \\ 0 & f_6/F_3 & (f_6+f_7)/F_3 \end{Bmatrix} \cdot 100,$$

where $F_1 = f_1 + 2f_1$, $F_2 = f_4 + 2(f_3 + f_5)$, $F_3 = f_7 + 2f_6$.

The overlap matrix is a measure of the quality of the group separation. It also indicates possible contaminations of groups.

This CLUCOV algorithm was widely used for the two-dimensional case. This revealed that the use of Gaussian functions to describe the distributions of the points is not a restriction when one is working with a program.

Table V shows how the cluster algorithm separated events. In this table, we also give the result of the iterative algorithm of Ref. 27. This result was obtained for five preliminary groups and after seven iterations. The solution was stable for a large range of the parameters t_s and t_c: $t_s = 0-0.25$ and $t_c = 0.2-0.55$.

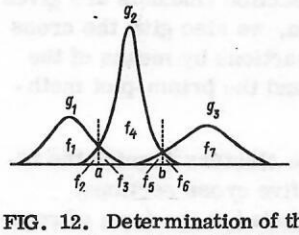

FIG. 12. Determination of the overlap matrix O_{ik} (12) for three groups characterized by the areas under Gaussian curves.

TABLE V. Dependence on the cluster type of the distribution of the number of events* generated by the Monte Carlo method for the reaction channels $K^+p \to K^*(890)p$, $K^+p \to K^*(1420)p$, and $K^+p \to \Delta(1236)K$ in the reaction $K^+p \to pK^0\pi^+$ at $p_{lab} = 5$ GeV/c.

Cluster	$K^*_{890}p$	$K^*_{1420}p$	$\Delta(1236)K$	Σ
500 Monte Carlo events				
1	15	12	261	288
2	189	0	0	189
3	0	21	0	21
not joined	0	0	2	2
Σ	204	33	263	500
2010 Monte Carlo events				
1	767	2	11	780
2	13	109	34	156
3	32	13	997	1042
not joined	5	6	21	32
Σ	817	130	1063	2010

*For the first set of data, the algorithm CLUCOV was used; for the second, the CERN interactive program of Ref. 20 was used.

2. APPLICATION OF THE CLUSTER ALGORITHM CLUCOV

The cluster algorithm CLUCOV for the reactions

$$\pi^+p \to p\pi^+\pi^+\pi^-, \quad p_{lab} = 16 \text{ GeV}/c; \qquad (13)$$
$$\pi^-p \to p\pi^+\pi^-\pi^-, \quad p_{lab} = 16 \text{ GeV}/c \qquad (14)$$

was used to make a systematic analysis of these reactions. The aim of using the cluster program for the reactions

$$K^-p \to pK^-\pi^+\pi^-, \quad p_{lab} = 10 \text{ GeV}/c; \qquad (15)$$
$$K^-p \to pK^0\pi^-\pi^0, \quad p_{lab} = 10 \text{ GeV}/c \qquad (16)$$

was to separate the subprocess $K^-p \to K^*(890)\Delta(1236)$ (as completely and cleanly as possible, which has hitherto been impossible by means of the ordinary methods) in order to obtain information about the production mechanism of these resonances.

Application of the Algorithm to the Reactions $\pi^+p \to p\pi^+\pi^+\pi^-$ at 16 GeV/c.[41] The reactions (13) and (14) are excellently suited to application of the algorithm CLUCOV, since there are seven independent kinematic variables. The analysis is already multidimensional, but the number of events is even greater: 19 178 events for the reaction (13) and 5166 events for (14). These reactions have also been investigated by other methods (prism-plot analysis, longitudinal-momentum analysis, maximal likelihood method), which gives the possibility of comparing the results.

A necessary step in each cluster analysis is the choice of the kinematic variables. The seven variables needed for the unique kinematic description of the four-particle reactions (13) and (14) were chosen in accordance with the following criteria[42-44]: Lorentz invariance of the description, invariance under permutations of the final particles up to a linear transformation that does not change the cluster structure, and invariance under permutation of the particles of the beam and the target.

These criteria are satisfied for the Yang variables. A detailed discussion and generalization of these variables is presented in Appendix 1. The six scalar products of the four-momenta are chosen:

$$\left.\begin{aligned} q_i &= (p_{\text{beam}} p_c), \quad i=1,\ 2,\ 3; \\ q_i &= (p_{\text{targ}},\ p_c), \quad i=4,\ 5,\ 6, \end{aligned}\right\} \tag{17a}$$

where $c=p,\ \pi_f^+,\ \pi_s^+$ for the reaction (12) and $c=p,\ \pi_f^-,\ \pi^+$ for the reaction (13) (the subscripts f and s denote the π meson with the larger and smaller c.m.s. longitudinal momentum, respectively). The seventh variable is the Gram determinant of the four-momenta of the final particles:

$$q_7 = \Delta_4 (p_p,\ p_{\pi_f^+},\ p_{\pi_s^\pm},\ p_{\pi^\mp}). \tag{17b}$$

Together with the general description of the algorithm, it is necessary to explain the actual application of the analysis. The preliminary procedure explained in Sec. 1 was used with $R=5$ and $R=4.5$.[3] This gave 84 and 63 preliminary groups in the reactions (13) and (14). It was found to be helpful to have as many "seed" points as possible and also preliminary groups such that a seed point is contained with high probability in each real group.

After the iterative procedure, some iterative steps were made with all the events. Some clusters were separated already at the start. The separation parameters were the overlap matrix (12) and the distributions of the masses, the four-momentum transfer, the longitudinal momentum, and the decay angles. After this, the groups were divided and combined according to the parameter t(8). To economize the computing time, some well-separated groups were removed and the analysis was continued. In the final stage of the analysis, the same iterative procedure was carried out with the complete statistics, so that the analysis did not depend on the temporary removal of the separated groups.

We obtained 22 clusters for the reaction (13) and 17 clusters for (14). For the physical interpretation of the groups, it is necessary to establish a correspondence with the reaction mechanisms. A physical characterization of the groups was obtained by means of the one- and two-dimensional distributions for all the groups.

The clear resonance signals of the spectra and the effective masses show that ~95% of the events contain resonances in the final state. The observed resonances make it possible to identify clusters with subprocesses, which subsequently provide the names for the clusters. Only three clusters of the reaction (13) and two of the reaction (14) did not contain significant signals of resonances. One of the clusters of the reaction (13) is characterized by events with protons emitted forward in the center-of-mass system. An analogous candidate for baryon exchange was not found in the reaction (14). In Table VI we give the coordinates of the centers and their deviations in the space of the Yang variables for some clusters associated with diffraction dissociation of the target. Comparing them for the π^+p and π^-p reactions, we find that six of the seven components differ in different clusters. This emphasizes the need for and the advantages of using the complete kinematic information. It is clear that in connection with the low $N^*(1470)$ mass the corresponding subprocess is close to the kinematic limit. For the Gram determinant q_7 (17b), as the seventh component, a general tendency to an increase of $\langle q_7 \rangle$ with increasing mass of the $p\pi\pi$ system is observed.

TABLE VI. Dependence of the positions of the centers of the clusters of the $p\pi\pi$ diffraction system on their masses in the reactions $\pi^+p \to p\pi_f^+\pi_s^+\pi^-$ and $\pi^-p \to p\pi^+\pi_f^-\pi_s^-$ at 16 GeV/c.*

Reaction	Number of events	q_1	q_2	q_3	q_4	q_5	q_6	q_7
$\pi^+p \to N^{*++}_{1470}\pi_f^+$ $\hookrightarrow \Delta^{++}_{1236}\pi_s^{0}\pi_s^{-+}$	1375	10.89	0.05	2.41	0.98	14.14	0.29	−0.04
		1.73	0.03	1.52	0.07	0.25	0.10	0.04
$\pi^-p \to N^{*+}_{1470}\pi_f^-$ $\hookrightarrow \Delta^{++}_{1236}\pi_s^{0}\pi_s^{-+}$	294	10.90	0.05	2.14	0.97	14.42	0.30	−0.04
		1.52	0.01	1.42	0.05	0.25	0.09	0.04
$\pi^+p \to N^{*++}_{1700}\pi_f^+$ $\hookrightarrow \Delta^{++}_{1236}\pi_s^{0}\pi_s^{-+}$	1595	9.44	0.11	2.44	1.13	13.80	0.38	−0.24
		2.18	0.07	1.54	0.18	0.30	0.17	0.24
$\pi^-p \to N^{*+}_{1700}\pi_f^-$ $\hookrightarrow \Delta^{++}_{1236}\pi_s^{0}\pi_s^{-+}$	620	9.44	0.11	2.49	1.14	13.98	0.35	−0.24
		2.33	0.09	1.58	0.20	0.35	0.15	0.28
$\pi^+p \to N^{*++}_{2040}\pi_f^+$ $\hookrightarrow p\pi_s^+\pi^-$	676	7.50	0.14	3.14	1.49	13.19	0.64	−1.16
		2.24	0.10	2.10	0.38	0.38	0.34	1.05
$\pi^-p \to N^{*+}_{2040}\pi_f^-$ $\hookrightarrow p\pi_s^+\pi^-$	217	9.02	0.14	2.58	1.27	13.32	0.66	−1.12
		2.39	0.11	1.77	0.29	0.44	0.33	1.11
$\pi^+p \to N^{*++}_{2400}\pi_f^+$ $\hookrightarrow p\pi_s^+\pi^-$	398	8.49	0.15	3.88	1.46	11.81	0.92	−5.94
		2.38	0.10	2.35	0.38	0.90	0.49	5.17
$\pi^-p \to N^{*+}_{2400}\pi_f^-$ $\hookrightarrow p\pi^+\pi_s^-$	94	5.50	0.09	4.88	1.86	12.77	0.66	−0.80
		2.05	0.05	2.88	0.48	0.41	0.37	0.82

*The upper row gives the coordinates of the center of the cluster; the lower gives their deviations.

It is perfectly natural that the component $\langle q_2 \rangle$ for these clusters does not increase, since q_2 is associated with transfer of four-momentum from the target to the diffraction $p\pi\pi$ system:

$$q_2 = m_\pi^2 - t/2.$$

The diffraction subprocesses selected here all have small values of t.

The cross sections of the reaction channels are given in Table VII. For comparison, we also give the cross sections obtained for these reactions by means of the maximal likelihood method[45] and the prism-plot method.[46,47]

Overlappings of two or three clusters require the introduction of corrections for five cross sections. These overlappings are manifested in the form of resonance signals in the invariant mass spectra that are not

[3] R is the Euclidean distance in the space $q_1, \ldots, q_7$ of (17) (the four-momenta are measured in GeV).

TABLE VII. Comparison of the cross sections of the subprocesses found by cluster analysis, the method of maximal likelihood,[24] and prism-plot analysis.[25]

Channels of the reactions $\pi^{\pm}p \to$	Cross section, μb					
	Cluster analysis		Method of maximal likelihood		Prism-plot analysis	
	π^+p	π^-p	π^+p	π^-p	π^+p	π^-p
1. $A_1^{\pm}p$ $\to \rho^0\pi^{\pm}$	200±22	220±18	280±67	294±56	590±29	619±40
2. $A_2^{\pm}p$ $\to \rho^0\pi^{\pm}$	200±26	136±23	167±40	158±33		
3. $A_3^{\pm}p$ $\to f\pi^{\pm}$, $\rho^0\pi^{\pm}$	114±28	106±16	115±27	113±22		
4. $A_4'p$ $\to \rho^0\pi^{\pm}$, $f\pi^{\pm}$	55±15	40±8	–	–		
5. $N^{*+}_{1470}\pi^{\pm}$ $\to \Delta^{++}_{1236}\pi^-+$	68±17	62±13	146±40	128±22	189±15	147±18
6. $N^{*+}_{1700}\pi^{\pm}$ $\to \Delta^{++}_{1236}\pi^-+$	115±18	128±15	106±27	117±22		
7. $N^{*+}_{2040}\pi^{\pm}$ $\to p\pi^+\pi^-$	48±12	45±8	–	–	77±11	166±19
8. $N^{*+}_{2400}\pi^{\pm}$ $\to p\pi^+\pi^-$	28^{+9}_{-13}	20±6	–	–		
9. $\Delta^{++}_{1236}\rho^0$	160±20	–	180^{+40}_{-27}	–	194±16	–
10. $\Delta^{++}_{1236}f$	108±17	–	73±13	–	98±12	–
11. $\Delta^{++}_{1236}g^0$	30±9	–	–	–	32±7	–
12. $\Delta^{++}_{1690}\rho^0$	40±10	–	–	–	67±10	–
13. $\Delta^{0}_{1236}\rho^0$	–	48±12	–	–	–	–
14. $\Delta^{0}_{1236}f$	–	11±4	–	–	–	–
15. $N^{*0}_{1520}\rho^0$	–	48±10	–	–	–	–
16. $N^{*0}_{1520}f$	–	19±5	–	–	–	–
17. $\Delta^{++}_{1236}\pi^{\pm}\pi^-$	35±15	80±19	106±28	127±26	–	44±10
18. $\Delta^{0}_{1236}\pi^{\pm}\pi+$	30±9	–	40±7	45±11	–	–
19. $N^{*0}_{1520}\pi^{\pm}\pi+$	18±5	–	–	–	–	–
20. $p\pi^{\pm}\rho^0$	63±34	29±10	47±15	68±14	–	90±15
21. $p\pi^{\pm}f$	10±8	–	27±11	40±13	–	30±9
22. $p\pi^{\pm}g^0$	6±5	15±7	–	–	–	–
23. p^*_L (proton) > 0	6±1	–	–	–	–	–
24. $p\pi^{\pm}\pi+\pi^-$	45±32	72±25	47±17	35±16	53±20	32±15

observed in the experiment.

The cross section for the processes $\pi^+p \to pA_3^+$ and $\pi^+p \to pA_2^+$ was changed by 11 ± 3 μb in accordance with the signal from A_2 seen in A_3 (Fig. 13).[4)]

We found a ρ^0 signal with cross section 15 ± 4 μB in the mass spectrum of the cluster $N^*(1470)$ having a clear $\Delta^{++}(1236)$ signal in the $p\pi_3^+$ mass spectrum. Therefore, a similar correction of the cross sections was made for the $N^*(1470)\pi$, $\Delta^{++}(1236)\rho$ and $\Delta^{++}(1236)f$ subprocesses.

The overlap matrices (12) of the reactions (13) and (14) (Tables VIII and IX) give a picture of the overlappings of the clusters in the seven-dimensional space of the Yang variables. A satisfactory separation of the clusters is observed.

To estimate the total errors of the cross sections in the cluster analyses, it is necessary to consider not only the statistical errors but also the errors due to residual contamination and irregular joining of points to clusters. To estimate this part of the error, we determined the changes in the joining of points to clusters as a result of some additional iterations of the cluster algorithm. The errors we present contain two parts. Comparing the cross sections of the diffraction dissociation process (processes 1 and 3–8 in Table VII) of the π^+p experiment with the corresponding process of the π^-p experiment, we find that they agree well. This is also true for the cross sections obtained by other methods. The total cross section of diffraction dissociation of the beam and target is the same for all the three methods.

The results for the A mesons require a more detailed discussion. In Ref. 48, there is an analysis of the partial waves of the 3π system of low mass in which the states A_1^+, A_2^+, A_3^+ are described by partial waves with spin and parity $J^P = 1^+$, 2^+, and 2^-. Strong interferences are also observed. However, the interferences do not occur in the formalism of the cluster analysis. The found clusters have maxima of the density in the phase space. If some elements of the overlap matrix differ appreciably from zero, this may be a consequence of interference of the corresponding subprocesses. However, one cannot take the values of the elements of the overlap matrix as a measure of the interference. By means of the cluster analysis, one can clearly separate two neighboring clusters even if there is strong interference of the corresponding subprocesses. Analysis of the partial waves gives for the 1^+ wave the cross section 333 ± 38 μb, for the 2^+ wave 48 ± 14 μb, and for the 2^- wave 119 ± 25 μb.

The comparison made in Table VII shows that the data for the three methods agree well only for A_3 production but in the case of the strongly interfering A_1 and A_2 waves only for their sum.

For the nondiffraction processes (see Table VII), the cross sections obtained by the different methods agree well. The differences are explained by the fact that the early analyses[46-48] did not take into account various subprocesses. However, the introduction of these subprocesses in the initial stage of the analysis does not permit one to find all the subprocesses of small cross section. The possible exchange of baryons [cluster 23 of the reaction (13)] was also not taken into account.

It follows from the law of isospin conservation that $\sigma(\pi^+p \to \Delta^{++})/\sigma(\pi^-p \to \Delta^0) = 9/1$. It can be seen from Table VII that this ratio is satisfied for $\pi p \to \Delta f$. However, the cross section for the process $\pi^-p \to \Delta^0(1236)\rho^0$ is twice the expected value. It must not be forgotton that this process was not found by other methods. For the subprocesses $\pi^-p \to \Delta^0(1236)$ and $\pi^-p \to \Delta^0(1890)\rho_0$, a cross section ~4 μb was expected. However, one can draw the conclusion that in the channel we consider with 5116 events, which has cross section 1.08 μb, the limit of detection for cluster analysis is approximately 4 μb. This could explain the absence in the reaction (14) of the baryon exchange group found in the reaction (13). We shall consider some particularly interesting clusters. Besides the effective mass distributions, the figures also show the distributions of the decay angles in the Jackson system.

For the $p\pi\pi$ and 3π systems, the z axis of the coordi-

[4)] The error in the choice of the background is not included in the error of the cross section.

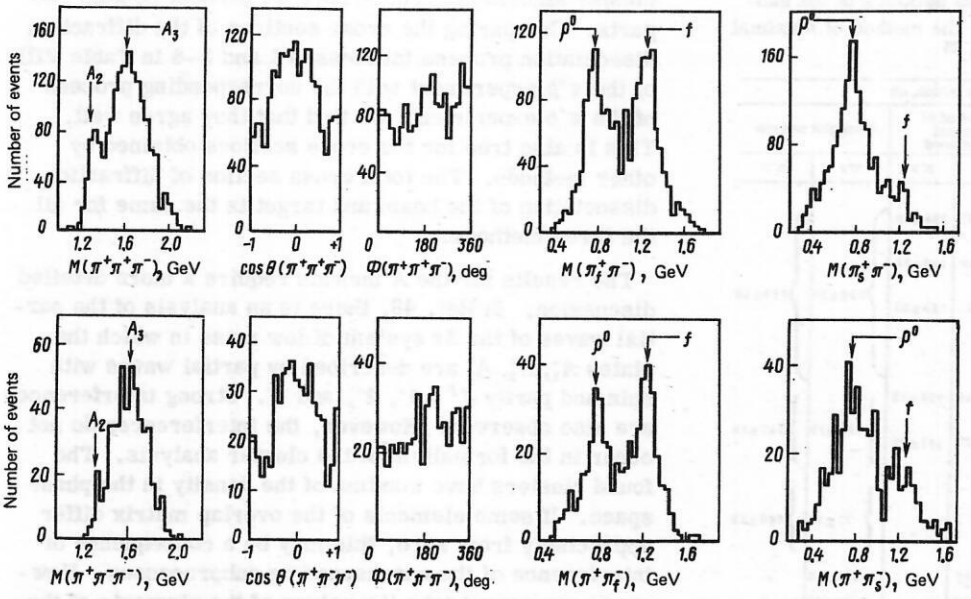

FIG. 13. Distributions of the effective masses and decay angles characterizing the channels $\pi^\pm p \to pA_3^\pm$ in the reaction $\pi^\pm p \to p\pi^\pm\pi^+\pi^-$ at $p_{lab} = 16$ GeV/c.

nate system is directed along the normal to the decay plane, and for the $p\pi$ and $\pi\pi$ systems along the direction of the proton and the π meson with negative charge of the beam.

The reactions $\pi^\pm p \to pA_3^\pm$. The overlapping of the channels $\pi^+p \to pA_3^+$ and $\pi^+p \to pA_2^+$ has already been considered (see Fig. 13). Of particular interest is the presence of a clear signal of the ρ^0 meson with the f meson in both $\pi^+\pi^-$ mass distributions. The ρ^0 signal cannot be explained by overlapping with pA_2^+. This confirms the assertion made in Ref. 50 that A_3 also decays through the channel $A_3^\pm \to \rho^0\pi^\pm$. A further indication of this decay is obtained in an analysis of the partial waves

TABLE VIII. Overlap matrix $O_{kk'}$ (12) for clusters in the reaction $\pi^+p \to p\pi_f^+\pi_s^+\pi^-$ at 16 GeV/c.

	A_1^+	A_1^+	A_2^+	A_3^+	A'^+	N^{*+} (1470)	N^{*+} (1700)	N^{*+} (2040)	"N^{*+} (2400)"	Δ^{++} (1236) ρ^0	Δ^{++} (1236) f	Δ^{++} (1236) g^0	Δ^{++} (1890) ρ^0	Δ^{++} (1236)	Δ^0 (1236)	N^{*0} (1520)	ρ^0	f	g^0	p_L^* (proton) < 0	$p\pi^+\pi^-$	$p\pi^+\pi^+\pi^-$
$p\pi^+\pi^+\pi^-$	99																	1	5			92
$p\pi^+\pi^+\pi^-$		97	2	1																	99	
p_L^* (proton) < 0			2	84	8						1									99		
g^0		1	92	5															93			2
f																		90	3			
ρ^0				1	88							5	2				82					
N^{*0} (1520)				1				2								88						
Δ^0 (1236)								1							82							
Δ^{++} (1236)								1				1		80			2					
Δ^{++} (1890) ρ^0													91		1		2	2				
Δ^{++} (1236) g^0												91		4								
Δ^{++} (1236) f				1			1				93	4		2			5					
Δ^{++} (1236) ρ^0						1				96	1											
"N^{*+} (2400)"								91								3						
N^{*+} (2040)								91	2				1	4	1							
N^{*+} (1700)							94	1						3	2							
N^{*+} (1470)						97	1			2												
A_4^+					88											4		4	7			
A_3^+			1	84	8						1				8	1	3					
A_2^+		1	92	5											1		2					
A_1^+		97	2	2																		
A_1^+	99		2																			

TABLE IX. Overlap matrix $O_{kk'}$ (12) for clusters in the reaction $\pi^- p \to p\pi^+\pi_f^-\pi_s^-$ at 16 GeV/c.

	A_1^-	A_2^-	A_3^-	A'^-	N^{*++} (1470)	N^{*++} (1700)	N^{*++} (2040)	"N^{*++} (2400)"	Δ^0 (1236) ρ^0	Δ^0 (1236) f	N^{*0} (1520) ρ^0	N^{*0} (1520) f	Δ^{++} (1236)	ρ^0	g^0	$p\pi^+\pi^-$	$p\pi^+\pi^-$
$p\pi^+\pi^-\pi^-$																2	84
$p\pi^+\pi^-\pi^-$											2		2	3	85		14
g^0														88	2		
ρ^0													91		9		
Δ^{++} (1236)			1				3						93				
N^{*0} (1520) f				1						88			1	2			
N^{*0} (1520) ρ^0			1	2			1			84		3	1				
Δ^0 (1236) f									88			1					
Δ^0 (1236) ρ^0								91									
"N^{*++} (2400)"							1	91									
N^{*++} (2040)				4			84	6			2		1		3		
N^{*++} (1700)						96	5						2				
N^{*++} (1470)					99	1											
A_4^-			1	77			1				3	2	1		2	1	
A_3^-			84	11			1			5	2		2				
A_2^-	1	85	8						1		3						
A_1^-	98	10							5								

of the reaction (13).[26]

The reaction $\pi^+ p \to \Delta^{++}(1236)\rho^0$ (Fig. 14). To estimate the number of subprocesses obtained by the cluster analysis, we show in Fig. 14 some properties of the cluster that we unambiguously identify with this reaction; it was studied in detail in Ref. 49. The $M(p\pi_s^+)$ and $M(\pi_f^+\pi^-)$ mass spectra have clear signals of the resonances $\Delta^{++}(1236)$ and $\rho^0(765)$ (see Fig. 14).

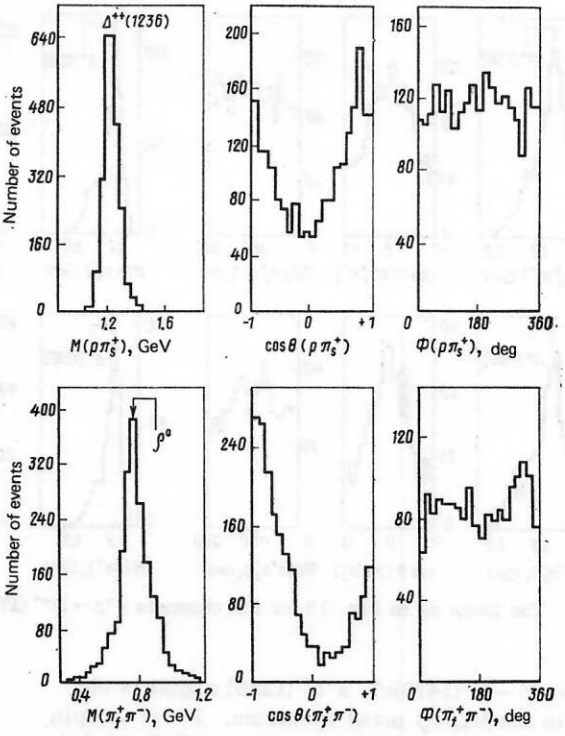

FIG. 14. The same as in Fig. 13 for the channel $\pi^+ p$ $\Delta^{++}(1236)\rho^0$ in the reaction $\pi^+ p \to p\pi^+\pi^+\pi^-$.

The asymmetry of the distribution with respect to the decay angle $\cos\theta(\pi_f^+\pi^-)$ can be explained by the interference between the production of ρ^0 and the s-wave background. The cross section of this subprocess agrees well with the values obtained by other methods (see Table VII).[49]

The reactions $\pi^\pm p \to p A_4^\pm(1900)$ (Fig. 15). Two $A_4(1900)$ decay channels have been found. The decay $A_4(1900) \to \pi\rho^0$ was found in Ref. 46. We found the decay $A_4(1900) \to f\pi$. The decay $A_4 \to g^0\pi$, which was indicated for the 3π system, was not found in this mass range.[51]

The reactions $\pi^\pm p \to N^*(1700)\pi^\pm$ (Fig. 16). For the diffraction system $N^*(1700)$, as for the sub-

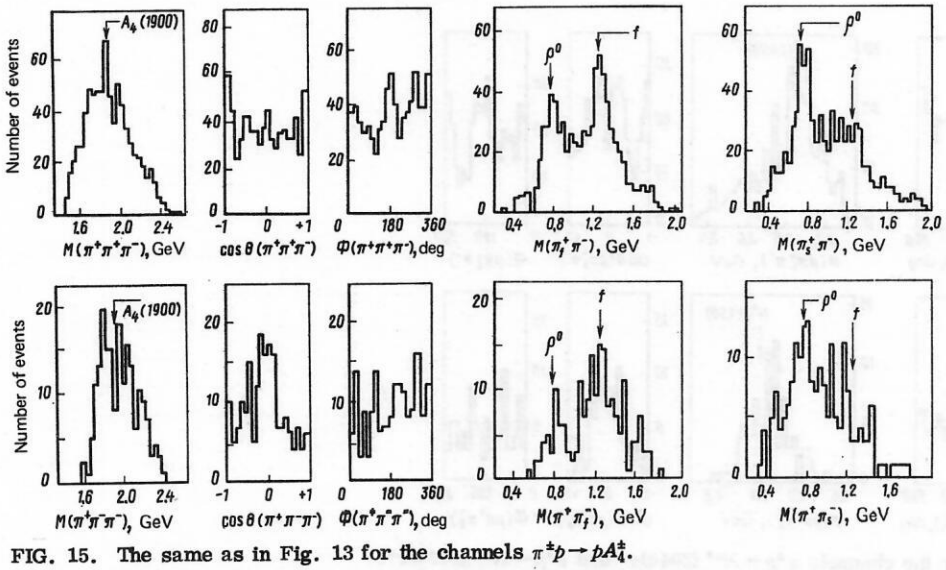

FIG. 15. The same as in Fig. 13 for the channels $\pi^\pm p \to p A_4^\pm$.

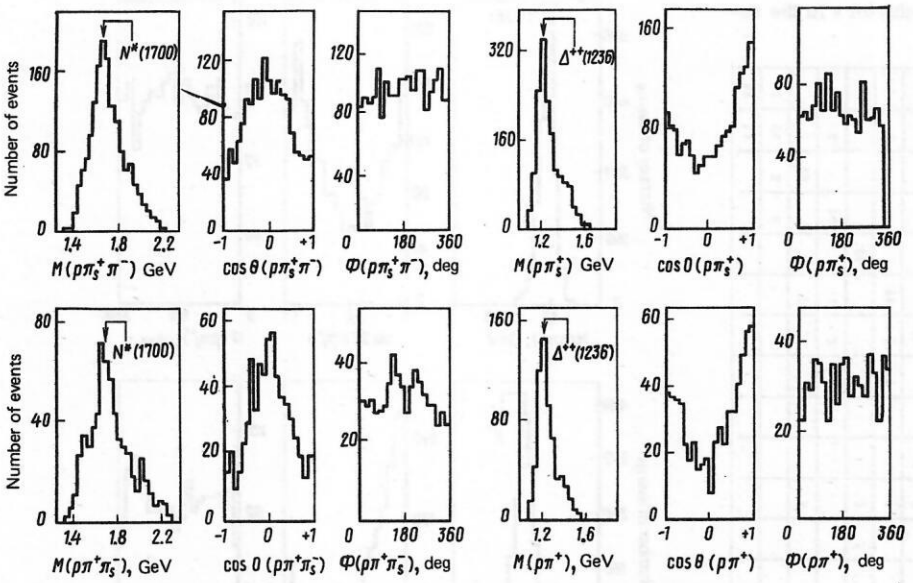

FIG. 16. The same as in Fig. 13 for the channels $\pi^{\pm}p \to N^{*+}(1700)\pi^{\pm}$.

process $\pi^{\pm}p \to N^*(1470)\pi^{\pm}$, a $\Delta^{++}(1236)$ signal is observed in the $M(p\pi_s^+)$ mass spectrum. From isospin conservation there follows the ratio $\sigma(\Delta^{++}\pi^-)/\sigma(\Delta^0\pi^-) = 9/1$ for the decays $N^*(1700) \to \Delta\pi$. The experimental distributions of the masses of the $p\pi$ system do not contradict this.

The reactions $\pi^{\pm}p \to N^*(2040)\pi^{\pm}$ and $\pi^{\pm} \to N^*(2400)\pi^{\pm}$ (Fig. 17). The cluster analysis gave two relatively small groups (see Table VI) characterized by a clear signal at large masses of the $p\pi\pi$ system. Production of $\Delta^{++}(1236)$ was not detected. Such signals have not yet been observed in the mass distributions of the $p\pi\pi$ system.[52] The approximation of these signals by a Breit–Wigner function gives the masses and widths $M_1 = 2.02 \pm 0.03$, $\Gamma_1 = 0.5 \pm 0.06$, $M_2 = 2.38 \pm 0.06$, $\Gamma_2 = 0.5 \pm 0.15$ GeV.

These signals were found in the reactions (13) and (14), which confirms the conjectured existence of the states $N^*(2040)$ and $N^*(2400)$. Because of the low statistical significance of these groups of events, the properties of these clusters need to be compared with others.

Study of the centers Q_i of these groups (see Table VI) makes it possible to regard the $N^*(2040)$ and $N^*(2400)$ systems as members of the series of diffraction systems $N^*(1470)$ and $N^*(1700)$. An argument for such an interpretation is the equality of the corresponding cross sections of the reactions (13) and (14) (see Table VII).

The 3π mass spectra of these clusters have a very high threshold, which rules out an interpretation of the $N^*(2040)$ and $N^*(2400)$ clusters as a kinematic reflection of interference effects in the three-pion system. From the distribution of the Jackson angle $\cos\theta_{GF}$ (see Fig. 17) it can be concluded that although cluster analysis does permit the detection of these subprocesses of small cross sections it does not in each case separate a complete and pure group of events.

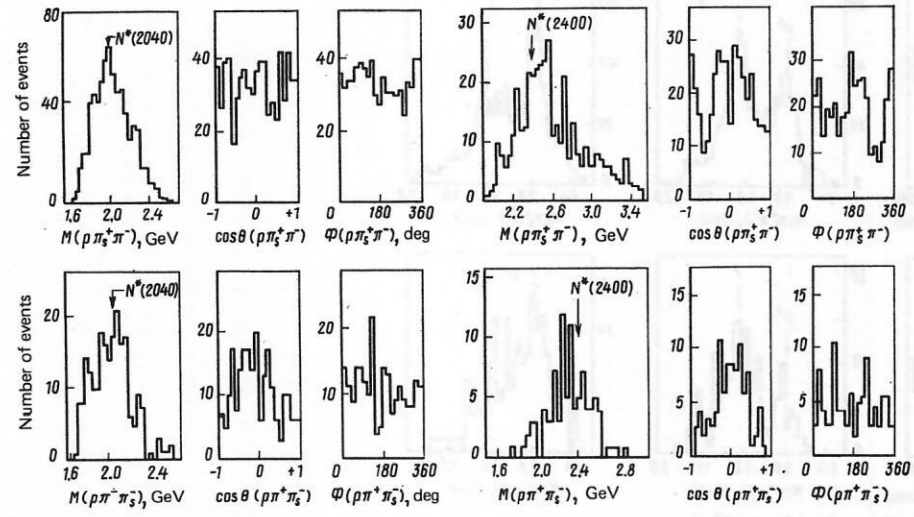

FIG. 17. The same as in Fig. 13 for the channels $\pi^{\pm}p \to N^{*+}(2040)\pi^{\pm}$ and $\pi^{\pm}p \to N^{*+}(2400)\pi^{\pm}$.

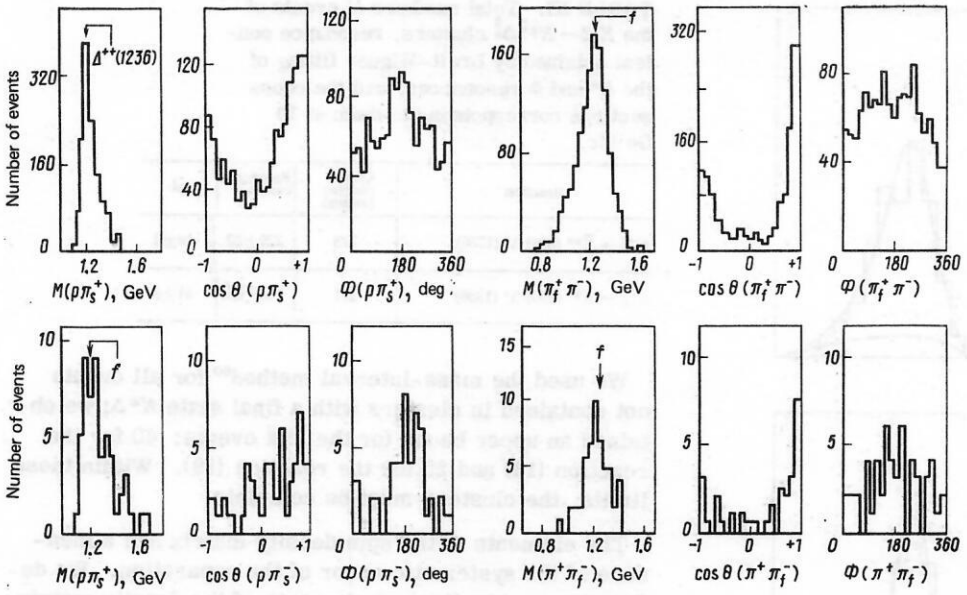

FIG. 18. The same as in Fig. 13 for the channels $\pi^{\pm}p \to \Delta^{++}_{0}(1236)f$.

The reactions $\pi^{\pm}p \to \Delta^{++}(1236)f$ (Fig. 18). For the $\pi^{+}p$ reactions, pure resonance signals are obtained in the corresponding mass spectra. The distributions of the decay angles also have the expected profiles. For the $\pi^{-}p$ reactions, because of the small cross section, there is no such clear picture.

The reaction $\pi^{+}p \to \Delta^{++}(1890)\rho^{0}$ (Fig. 19). Here too clear resonance signals are observed in the corresponding mass spectra. It was not possible to find the reaction $\pi^{-}p \to \Delta^{0}(1890)\rho^{0}$.

Application of Cluster Analysis to the Reactions $K^{-}p \to pK^{0}_{S}\pi^{\pm}\pi^{0}$ at 10 GeV/c.[53] In the study of the double resonance reactions[54-58]

$$K^{-}p \to \overline{K^{*0}}(890)\,\Delta^{0}(1236); \quad (18)$$
$$K^{-}\pi^{+} \hookleftarrow \quad \hookrightarrow p\pi^{-}$$
$$K^{-}p \to K^{*-}(890)\,\Delta^{+}(1236) \quad (19)$$
$$\overline{K^{0}}\pi^{-} \hookleftarrow \quad \hookrightarrow p\pi^{0}$$

the following difficulties were encountered: Clear signals of the resonances $K^{*}(890)$ and $\Delta(1236)$ were not obtained; contaminations from the diffraction dissociation of the beam or target particles remained; and the symmetry requirements on the distributions of the decay angles of the investigated resonances were not satisfied.

We therefore attempted to separate the reactions (18) and (19) at 10 GeV/c by means of cluster analysis. The obtained reaction cross sections and the numbers of events were

$K^{-}p \to pK^{-}\pi^{+}\pi^{-}$, $\sigma = 845 \pm 20\,\mu$b, 10074 events;

$K^{-}p \to p\overline{K^{0}}\pi^{-}\pi^{0}$, $\sigma = 652 \pm 5\,\mu$b, 2642 events.

Yang variables were chosen as a complete system of independent kinematic variables.

Properties of the K^{*} and Δ clusters. We now study the completeness and purity of the groups of events obtained in this manner.

The $K\pi$ and $p\pi$ mass distributions of both clusters give clear K^{*} and Δ signals (Fig. 20). All the other mass distributions, including the $p\pi\pi$ and $K\pi\pi$ spectra, are free from all symptoms of contamination.

Parity conservation in the strong decay of the K^{*} and Δ resonances gives a necessary condition for the purity and completeness of the groups of events:

$$\langle \mathrm{Im}\, Y_L^M \rangle = 0 \quad \text{for all } L \text{ and } M.$$

Here

$$\langle \mathrm{Im}\, Y_L^M \rangle = \int W(\cos\theta, \Phi)\, Y_L^M(\cos\theta, \Phi)\, d\Omega$$

and $W(\cos\theta, \Phi)$ is the distribution of the decay angles, for which parity conservation requires[59]

$$W\cos(\theta, \Phi) = W(\cos\theta, -\Phi); \quad W(\cos\theta, \Phi) = W(-\cos\theta, \Phi + \pi).$$

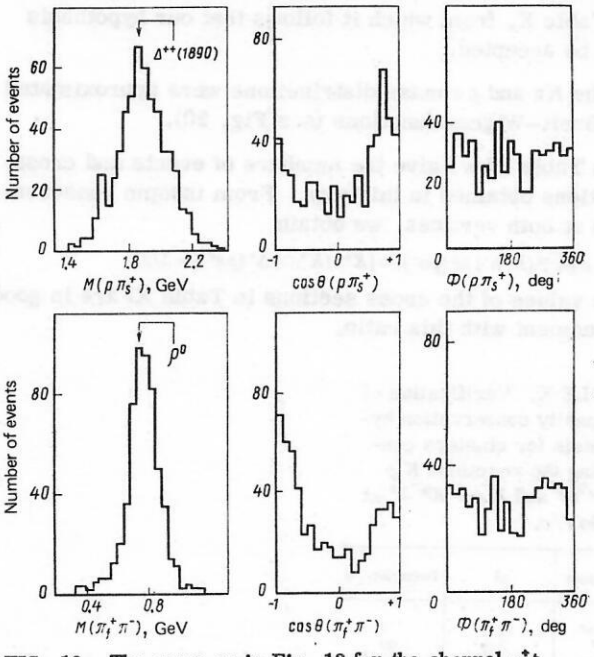

FIG. 19. The same as in Fig. 13 for the channel $\pi^{+}p \to \Delta^{++}(1890)\rho^{0}$.

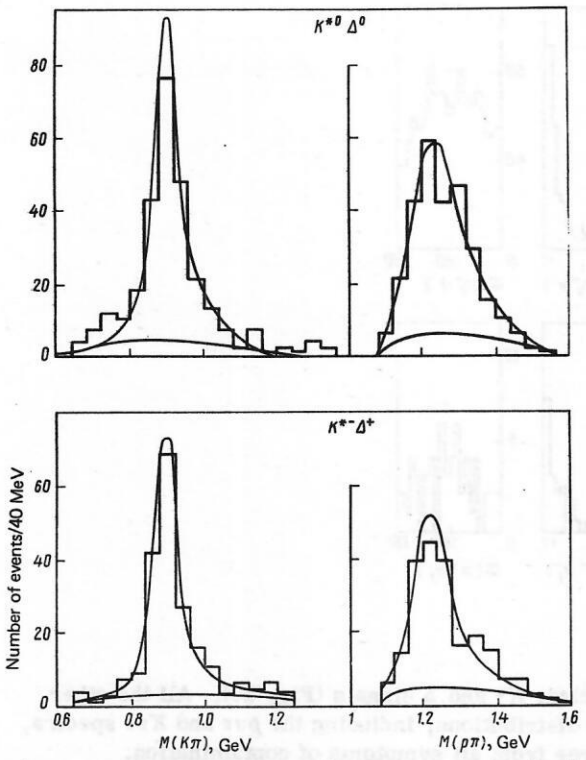

FIG. 20 Distributions of the effective masses for the channels $K^-p \to K^{*0}(1890)\Delta^+(1236)$ in the reaction $K^-p \to pK^0\pi^0\pi^-$ at $p_{lab} = 10$ GeV/c.

We determine χ^2 to test the parity conservation hypothesis for the groups of events:

$$\chi^2 = \sum_{L=1}^{L_{max}} \sum_{M=0}^{L} \left[\frac{\langle \mathrm{Im}\, Y_L^M \rangle}{\Delta(\mathrm{Im}\, Y_L^M)} \right]^2 .$$

It is assumed that the moments $\langle \mathrm{Im}\, Y_L^M \rangle$ are independent and distributed in accordance with a Gaussian law with error $\Delta(\mathrm{Im}\, Y_L^M)$. For $L_{max} = 4$ (and, therefore, nine degrees of freedom) we obtain the values for χ^2 given in Table X, from which it follows that our hypothesis can be accepted.

The $K\pi$ and $p\pi$ mass distributions were approximated by Breit–Wigner functions (see Fig. 20).

In Table XI we give the numbers of events and cross sections obtained in this way. From isospin conservation at both vertices, we obtain

$$\sigma[\bar{K}^{*0}(K^-\pi^+)\Delta^0(p\pi^-)]/\sigma[K^{*-}(\bar{K}^0\pi^-)\Delta^+(p\pi^0)] = 1/2.$$

The values of the cross sections in Table XI are in good agreement with this ratio.

TABLE X. Verification of the parity conservation hypothesis for clusters containing the reactions $K^-p \to \bar{K}^{*0}\Delta^0$ and $K^-p \to K^{*-}\Delta^+$ at 10 GeV/c.

Resonance	χ^2	Probability, %
$\bar{K}^{*0}$	14.9	9
Δ^0	5.6	80
K^{*-}	14.5	10
Δ^+	6.3	70

TABLE XI. Total numbers of events of the $K^-p \to K^{*0}\Delta^0$ clusters, resonance content obtained by Breit–Wigner fitting of the K^* and Δ resonances, and the cross sections corresponding to them at 10 GeV/c.

Reaction	Cluster content (events)	Resonance events	σ, μb
$K^-p \to \bar{K}^{*0}(890)\Delta^0(1236)$	278	226±22	19±2
$K^-p \to K^{*-}(890)\Delta^+(1236)$	211	168±25	41±8

We used the mass-interval method[60] for all events not contained in clusters with a final state $K^*\Delta$; we obtained an upper bound for the lost events: 40 for the reaction (18) and 25 for the reaction (19). Within these limits, the clusters must be complete.

The elements of the spin density matrix are a measure of the systematic error of the separation. We define the combinations of elements of the density matrix

$$\rho^+ = \rho^{11} + \rho^{1-1};$$
$$\rho^- = \rho^{00} + \rho^{11} - \rho^{1-1}.$$

One can show[61] that these combinations do not depend on the choice of the quantization axis, so that they must coincide in the helicity (s channel) and Jackson (t channel) systems. Figure 21 shows ρ^+ as a function of the four-momentum transfer t. At large $|t|$, the elements of the density matrix in the two systems are not equal. It follows that complete identification of the clusters with the $K^-p \to K^*\Delta$ process is impossible. The difference arises at large $|t|$; ρ^+ and ρ^- correspond to the part of the cross section that decreases exponentially with t. Therefore, the discrepancy affects only a small fraction of the events, and the integral conditions may be satisfied.

Overlapping of $K^*\Delta$ clusters. We now attempt to find the reasons for the incompleteness and impurity of the clusters. For this, we consider the cluster that in accordance with the overlap matrix (12) overlaps maximally with the $\bar{K}^{*0}\Delta^0$ and $K^{*-}\Delta^+$ clusters. These neighboring clusters have the following characteristics: The dominant process is $K^-p \to Q^-p$, which can be seen from the mass spectra; like the $K^*\Delta$ clusters, they are objects of low dimensionality in the

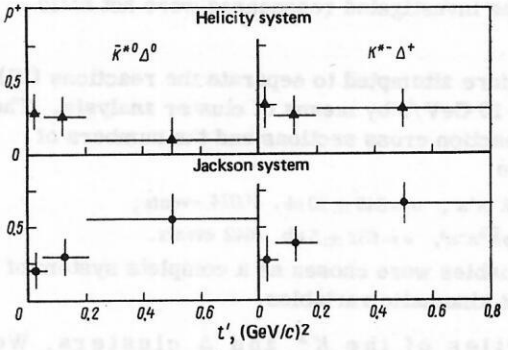

FIG. 21. Combination of the elements of the spin density matrix $\rho^+ = \rho^{11} + \rho^{1-1}$ for the reactions $K^-p \to K^{*0}(890)\Delta^0(1236)$ at $p_{lab} = 10$ GeV/c in the Jackson and helicity coordinate systems as a function of $t' = |t - t_{min}|$.

TABLE XII. Geometrical characterization of the $K^*\Delta$ clusters and the neighboring overlapping clusters.*

Process	$K^-p \to K^{*-}(890)\Delta^+(1236) \to p\bar{K}^0\pi^-\pi^0$							
Number of events	188							
Coordinate axes	$a1$ GeV²	$a2$ GeV²	$a3$ GeV²	$b1$ GeV²	$b2$ GeV²	$b3$ GeV²	Z GeV⁸	Eigenvalues
Center of gravity	7.41	0.43	0.21	0.99	5.59	3.40	−0.08	
$E1$	1.00	0.01	0.00	−0.03	−0.02	0.00	0.00	0.90
$E2$	0.00	0.75	0.00	0.00	0.36	0.32	−0.45	0.00
$E3$	0.00	0.07	0.91	−0.03	0.14	0.15	0.34	0.00
$E4$	0.03	−0.12	0.00	0.97	0.13	0.13	0.00	0.00
$E5$	−0.01	−0.03	−0.01	0.00	−0.70	0.71	0.00	6.74
$E6$	−0.02	0.52	−0.15	−0.22	0.56	0.58	0.00	0.01
$E7$	0.00	0.38	−0.38	0.01	0.14	0.11	0.82	0.01

Process	$K^-p \to \bar{K}^{*0}(890)\Delta^0(1236) \to pK^-\pi^+\pi^-$							
Number of events	278							
Coordinate axes	$a1$ GeV²	$a2$ GeV²	$a3$ GeV²	$b1$ GeV²	$b2$ GeV²	$b3$ GeV²	Z GeV⁸	Eigenvalues
Center of gravity	7.24	0.41	0.21	0.99	5.52	3.49	−0.04	
$E1$	1.00	−0.02	−0.01	−0.04	0.00	0.01	0.00	1.23
$E2$	0.04	0.80	0.00	0.35	−0.32	−0.36	−0.00	0.01
$E3$	0.01	0.00	1.00	0.00	−0.01	0.01	0.00	0.01
$E4$	0.03	−0.40	0.00	0.91	−0.01	0.01	0.00	0.00
$E5$	0.00	−0.03	0.01	0.00	0.71	0.70	0.00	7.35
$E6$	0.01	0.43	0.00	0.19	0.63	0.62	0.00	0.00
$E7$	0.00	0.00	0.00	0.00	0.00	0.00	1.00	0.00

Process	$K^-p \to Q^-p \to p\bar{K}0\pi^-\pi^0$							
Number of events	306							
Coordinate axes	$a1$ GeV²	$a2$ GeV²	$a3$ GeV²	$b1$ GeV²	$b2$ GeV²	$b3$ GeV²	Z GeV⁸	Eigenvalues
Center of gravity	8.64	0.49	0.15	0.92	3.68	4.34	−0.09	
$E1$	0.94	−0.19	−0.14	0.00	−0.01	0.01	0.22	0.02
$E2$	0.11	0.97	0.00	0.00	0.13	0.05	0.04	0.00
$E3$	0.14	−0.03	0.99	0.00	−0.01	0.01	0.03	0.00
$E4$	0.00	0.00	0.00	1.00	0.00	0.00	0.00	0.00
$E5$	0.01	−0.07	0.01	0.00	0.75	−0.65	−0.04	1.74
$E6$	−0.04	−0.12	0.00	0.00	0.64	0.75	0.04	0.39
$E7$	−0.23	0.00	0.00	0.00	0.00	−0.06	0.97	0.00

Process	$K^-p \to Q^-p \to pK^-\pi^+\pi^-$							
Number of events	881							
Coordinate axes	$a1$ GeV²	$a2$ GeV²	$a3$ GeV²	$b1$ GeV²	$b2$ GeV²	$b3$ GeV²	Z GeV⁸	Eigenvalues
Center of gravity	8.52	0.44	0.25	0.96	5.11	2.93	−0.13	
$E1$	0.96	−0.04	−0.08	−0.02	0.15	0.13	0.18	0.07
$E2$	0.08	0.71	0.69	0.00	0.02	0.00	0.01	0.01
$E3$	0.03	−0.69	0.71	−0.11	−0.03	0.03	0.03	0.01
$E4$	0.06	−0.08	0.08	0.97	0.00	0.00	−0.22	0.00
$E5$	−0.02	−0.04	0.02	0.00	0.72	−0.70	0.00	4.72
$E6$	−0.20	0.00	0.00	0.02	0.68	0.70	0.01	0.20
$E7$	−0.16	0.00	0.00	0.23	−0.04	−0.03	0.96	0.01

*The meaning of the given quantities is explained in Appendix 1.

phase space—more precisely, they have only two of the seven possible dimensions; their centers are close; the lengths and directions of the principal axes determined by the covariation of the ellipsoid determine the mutual penetration of the bunches. The low dimensionality of the clusters (two eigenvalues that are large compared with the remainder) makes it possible to illustrate different situations in phase space.

In Table XII we give for the $K^*\Delta$ clusters and their largest neighbors the numbers of events, the centers, the directions of the eigenvectors, and the eigenvalues (corresponding to the eigenvectors). For the process (18), as for the process (19), the neighboring clusters are disks oriented vertically with respect to the disk of the $K^*\Delta$ clusters and touching it. We project the points of one cluster onto the plane defined by the eigenvectors associated with the two largest values (principal plane). This projection illustrates the internal structure of the cluster.

To elucidate the question of the overlapping of two clusters, it is necessary to take into account the distance between their centers, the directions of the principal axes, and also structure not included in the approximation of multidimensional Gaussian distribution. For this, we project the points of one cluster onto the principal plane of the neighboring cluster. The center of the coordinate system is placed at the center of the cluster onto whose principal plane we project. In this way we obtain the projections of the $\overline{K^{*0}}\Delta^0$ cluster (Fig. 22) and $K^{*-}\Delta^+$ cluster (Fig. 23). They clearly show the overlapping of the process $K^-p \to K^*\Delta$ with the process $K^-p \to Q^-p$, so that this is a real overlapping in the multidimensional space, and no method using sections in phase space can separate this mechanism cleanly. This does not depend on the choice of the variables or the definition of distance.

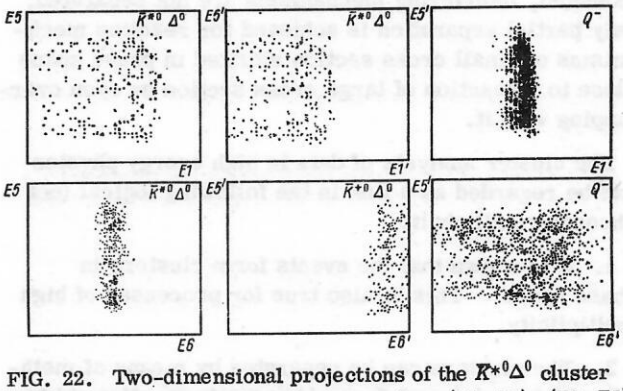

FIG. 22. Two-dimensional projections of the $\bar{K}^{*0}\Delta^0$ cluster onto the planes formed by the eigenvectors ($E1$, $E5$), ($E6$, $E5$), and ($E1'$, $E5'$), ($E6'$, $E5'$), and also two-dimensional projections of the $Q^- \to \bar{K}^{*0}\pi^-$ cluster onto the eigenplanes ($E1'$, $E5$) and ($E6'$, $E5'$): $\angle E1, E1' = 15°$; $\angle E5, E5' = 1°$; $\angle E6, E6' = 30°$.

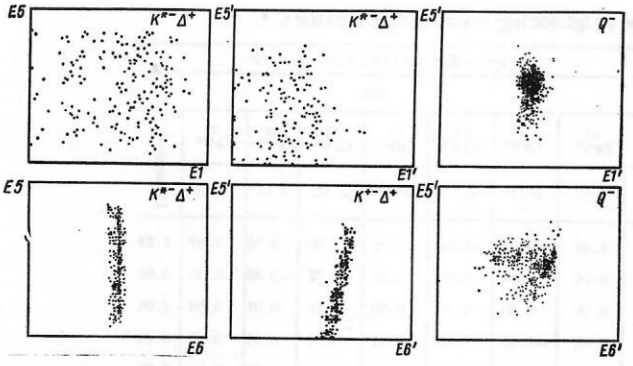

FIG. 23. The same as in Fig. 22 for the $K^{*-}\Delta^{+}$ and $Q \to K^{*-}\pi^{0}$ clusters: $\angle(E1, E1') = 20°$; $\angle(E5, E5') = 5°$; $\angle(E6, E6') = 30°$.

CONCLUSIONS

In analyzing exclusive experiments, different methods are used with the aim of elucidating which reaction mechanisms give a particular final state and determining the groups of events containing a known reaction mechanism for a further detailed study of this mechanism. In such analyses, it is necessary to use complete kinematic information (which we have for exclusive experiments). The dimensionality of the phase space of an n-particle final state is $3n-5$, which creates a number of methodological difficulties. All the methods proposed to overcome these difficulties assume that the reactions have a certain structure of the $(3n-5)$-dimensional distribution of the events in the phase space.

Cluster analyses of the distribution of points in the multidimensional space are a method for determining the structure of these distributions with the minimal number of assumptions. Application of two such methods of cluster analysis gave the following results: The obtained clusters are not separated by sections of the phase space with respect to some of the variables; a large fraction of the clusters contain resonances which enable one to establish an unambiguous correspondence between the clusters and the reaction mechanism; hitherto unknown reaction mechanisms have been found; there are indications of the existence of diffraction states of the $p\pi\pi$ system; cross sections have been obtained for all the reaction mechanisms. As was to be expected, interfering mechanisms are not separated; only partial separation is achieved for reaction mechanisms of small cross section situated in phase space close to a reaction of large cross section or even overlapping with it.

The cluster analysis of data in high energy physics can be regarded as a link in the following logical (not chronological) chain.

1. It is shown that the events form clusters in phase space. This is also true for processes of high multiplicity.

2. The clusters can be separated by means of methods which are almost free of parameters. Unambiguous identification of the clusters with dynamical mechanisms is not possible in all cases. One can obtain not only information about the distribution of the events in phase space but also indications of dynamical mechanisms of small cross sections.

3. The group of events (mechanisms) found and separated in this manner can then be studied in detail in the region of phase space in which they are situated (for example, one can make a partial-wave analysis).

4. These results are initial data for multi-channel analysis. They enable one not only to take into account the overlappings of different mechanisms but also to determine the relative phases between individual dynamical mechanisms.

The development of the methods of multidimensional analysis is still far from complete. Interesting results are to be expected from their application to inclusive reactions and to the search for jets.

The results of the present paper were obtained during many years of fruitful collaborations with Professor K. Lanius, H. E. Roloff, H. Böttcher, W. D. Nowak, P. Kostka, L. Becker, and T. Naumann.

I thank T. Naumann for preparing the draft in Russian.

APPENDIX I

Choice of the Kinematic Variables; Yang and their Generalization.[62] The results of a cluster analysis depend on the choice of the variables. It is therefore necessary to seek conditions that determine as unambiguously as possible the variables from a physical point of view. One can, for example, require that a complete set of variables be Lorentz-invariant and symmetric under permutation of the particles. The reaction

$$a+b \to 1+2+\ldots+n \tag{A1}$$

can be described by the invariant variables

$$(ai)=(p_a p_i);\ (bi)=(p_b p_i);\ (ik)=(p_i p_k). \tag{A2}$$

The number of variables (A2) is greater than the number of independent variables $(3n-5)$ at constant energy, and therefore some of them must be eliminated. For this, we require quasipermutational invariance between the particles $1,\ldots,n$ and invariance under replacement of particle a by b. Quasipermutational invariance means that any permutation of the final particles gives rise to only a linear transformation of the final particles. Linear transformations do not change the results obtained by the CLUCOV algorithm, so that is reasonable to require fulfillment of these two invariance conditions.

For four final particles, Yang[42] proposed the set of variables

$$n=4:\ (a1),\ (a2),\ (a3);\ (b1),\ (b2),\ (b3);\ \Delta_4(1234), \tag{A3}$$

where Δ_4 is the Gram determinant, having the form

$$\Delta_K(12\ldots K)=\begin{vmatrix}(11)\ldots(1K)\\ \vdots\\ (K1)\ldots(KK)\end{vmatrix}.$$

In a generalization of the variables (A3), it must be borne in mind that the invariants (A2) must satisfy the conditions

$$\sum_{i,k=1}^{n}(ik)=\text{const};\qquad\text{(A4a)}$$

$$\sum_{i=1}^{n}(ai)=\text{const};\qquad\text{(A4b)}$$

$$\sum_{i=1}^{n}(bi)=\text{const};\qquad\text{(A4c)}$$

$$\Delta_K(1\ldots K)=0,\quad\text{if}\quad K\geqslant 5.\qquad\text{(A4d)}$$

The condition (A4a) contains $n(n-1)/2$ variables; it is possible only for $n(n-1)/2\leqslant 3n-5$ (i.e., for $n\leqslant 5$). The Gram determinant Δ_K contains $K(K-1)/2$ variables. Therefore, the condition (A4d) is possible for $K(K-1)/2\leqslant 3n-5$. If we take into account (A4b) and (A4c), we obtain the following generalization of the set (A3):

$$\left.\begin{array}{l}(a1),(a2),\ldots,(a,n-1);\\(b1),(b2),\ldots,(b,n-1).\end{array}\right\}\qquad\text{(A5)}$$

It only remains to find a generalization of the determinant Δ_4. Consider the eigenvalues of the matrix $A_{ik}=(ik)$ (Ref. 32):

$$\lambda^n-\bar{\Delta}_1\lambda^{n-1}-\bar{\Delta}_2\lambda^{n-2}-\bar{\Delta}_3\lambda^{n-3}-\bar{\Delta}_4\lambda^{n-4}=0,\qquad\text{(A6)}$$

where λ denotes an eigenvalue and

$$\bar{\Delta}_m=(-1)^{m+1}\sum_{i_1,\ldots,i_m=1,\ldots,n}\Delta_m(i_1\ldots i_m).$$

By definition, the Δ_m are invariant under permutation of the final particles and can serve as a generalization of the determinant Δ_4 for a larger number of particles in the final state. In order to have all variables of the same dimension, we define further

$$Z_m^{(n)}=[(-1)^{m+1}\sum_{i_1,\ldots,i_m=1,\ldots,n}\Delta_m(i_1\ldots i_m)]^{1/m}.\qquad\text{(A7)}$$

Since $Z_1^{(n)}=\sum_{i=1}^{n}m_i^2$ is constant, only $Z_2^{(n)}$, $Z_3^{(n)}$, and $Z_4^{(n)}$ can serve as variables which are invariant under permutation of the final particles.

For $n=3,4,5,6$, we thus obtain the following sets of variables that are invariant in the indicated sense:

$n=3$: $(a1)$, $(a2)$;
$(b1)$, $(b2)$;

$n=4$: $(a1)$, $(a2)$, $(a3)$; $(b1)$, $(b2)$, $(b3)$; } Yang variables
$Z_4^{(4)}$;

$n=5$: $(a1),\ldots,(a4)$;
$(b1),\ldots,(b4)$;
$Z_4^{(5)}$, $Z_5^{(5)}$;

$n=6$: $(a1),\ldots,(a5)$;
$(b1),\ldots,(b5)$;
$Z_4^{(6)}$, $Z_5^{(6)}$, $Z_6^{(6)}$.

We note some properties of the quantities $Z_m^{(n)}$. Each of the $\binom{n}{m}$ terms of the sum (A7) is positive within the physical region. On the boundary of the physical region, $\Delta_m=0$ (Ref. 63). Generally speaking, not all the Δ_m in the variable $Z_m^{(n)}$ can vanish simultaneously. We therefore obtain $Z_{m,\min}^{(n)}\geqslant 0$. If we ignore the masses of the final particles, the boundaries of the physical region of the variables $Z_m^{(n)}$, which are proportional to $s=(p_a+p_b)^2$, are

$$Z_{2\min}^{(n)}=s/\sqrt{2n(n-1)};\quad Z_{2\max}^{(n)}=s/2;$$

$$Z_{3\min}^{(n)}=0;\quad Z_{3\max}^{(n)}=s\,[(n-2)/3n^2(n-1)^2]^{1/3};$$

$$Z_{4\min}^{(n)}=0;\quad Z_{4\max}^{(n)}=s\,[(n-2)(n-3)/8n^3(n-1)^3]^{1/4}.$$

APPENDIX 2

Classification in the Cluster Algorithm. It is assumed that $p(x)$, the distribution of N points x, is a superposition of distributions of K classes. Suppose the k-th class ω_k $(k=1,\ldots,K)$ has probability $p(\omega_k)$. Then the probability distribution is $p(x)=\sum_{k=1}^{K}p(\omega_k)\times p(x\,|\,\omega_k)$ where $p(x\,|\,\omega_k)$ is the conditional probability distribution of the points x belonging to class k. The minimum-risk solution is obtained as follows.

For a given point x, we find in accordance with Bayes's rule the conditional probability of belonging to class k:

$$p(\omega_k|x)=p(x|\omega_k)\,p(\omega_k)\Big/\sum_{i=1}^{k}p(x|\omega_i)\,p(\omega_i)$$

and we join the point x to the class that has the maximal value of $p(\omega_k|x)$.

If $p(\omega_k|x)$ is a multidimensional Gaussian distribution, we obtain the rule (11) and the weight of the expression (10). The algorithm CLUCOV is a classification procedure in which the *a priori* probabilities $p(\omega_k)$ and the parameters $\bar{X}^k$ and C^k of the distributions $p(x\,|\,\omega_k)$ are replaced by better estimates from iteration to iteration.

[1]S. Brandt *et al.*, Phys. Lett. **12**, 57 (1964).
[2]H. Schiller, Preprint Zeuthen-PHE 72-8, Berlin (1972).
[3]P. Kostka *et al.*, Nucl. Phys. **B86**, 1 (1975).
[4]M. C. Forster *et al.*, Phys. Rev. **D6**, 3135 (1972).
[5]R. G. Glasser *et al.*, Phys. Lett. **B53**, 387 (1974).
[6]T. Ludlam and R. Slansky, Phys. Rev. **D8**, 1408 (1973).
[7]E. L. Berger *et al.*, Phys. Lett. **B43**, 132 (1973).
[8]J. E. Brau *et al.*, Phys. Rev. Lett. **27**, 1181 (1971); A. Ferrando *et al.*, Preprint CERN/EP/PHYS 77-54 (1977).
[9]A. Ferrando *et al.*, Nucl. Phys. **B92**, 61 (1975).
[10]Experiments at CERN in 1977, CERN Scientific Information Service (1977).
[11]A. K. Wroblewski, Rapporteur's talk at the Fifteenth Intern. Conf. on High Energy Physics, Kiev (1970); D. R. O. Morrison, CERN/EP/PHYS 76-45; Invited talk at a theoretical session at the Seventh Intern. Colloquium on Multiparticle Reactions, Tutzing (1976); K. J. Biebl *et al.*, Nucl. Phys. **B102**, 120 (1976).
[12]W. Kittel, Summary talk at the Intern. Symposium on Antinucleon-Nucleon Interactions, Prague-Liblice (1974).
[13]L. Van Hove, Phys. Lett. **B28**, 429 (1969); Nucl. Phys. **B9**, 331 (1969).
[14]H. Bötcher, Preprint Zeuthen-PHE 74-2; in: Proc. of the Fifth Intern. Symposium on Many Particle Hadrodynamics, Eisenach-Leipzig (1974).
[15]M. Deutschmann *et al.*, Nucl. Phys. **B50**, 61, 80 (1972).
[16]H. E. Roloff, Math. Nat. Diss. A (1976).
[17]E. L. Berger, Phys. Lett. **B43**, 132 (1973).
[18]F. T. Dao *et al.*, Phys. Lett. **B45**, 73 (1973).
[19]T. Ludlam and R. Slansky, Phys. Rev. **D8**, 1408 (1973).
[20]J. Haulon *et al.*, Phys. Lett. **B46**, 415 (1973).
[21]T. Ludlam *et al.*, Phys. Lett. **B48**, 449 (1974).
[22]M. R. Anderberg, Cluster Analysis for Applications, New York (1973); B. Schorr, Preprint CERN/DD Int/76-3.
[23]C. T. Zahn, IEEE Trans. Comput. C-20 **20**, 68 (1971).
[24]D. J. Schotanus, in: Proc. of the Topical Meeting on Multidimensional Data Analysis, CERN (1976).
[25]W. Kittel, Invited paper at the Fourth Intern. Winter Meeting on Fundamental Physics, Salardü, Spain (1976).
[26]T. Ludlam and R. Slansky, Phys. Rev. **D16**, 100 (1977).
[27]E. S. Gelsema, Preprint CERN/DD/74-16 (1974).
[28]M. Baubillier *et al.*, "Multidimensional analysis of the reaction $\pi^-n\to\pi^-\pi^-\pi^+n$ at 9 GeV/c," Submitted to the Intern. Conf. on High Energy Physics, Budapest (1977).
[29]M. Baubillier *et al.*, "A multidimensional analysis of the

coherent reaction $\pi^- d \to \pi^- \pi^- \pi^+ d$ at 9 GeV/c," Submitted to the Intern. Conf. on High Energy Physics, Budapest (1977).
[30]Ch. De la Vaissierz, in: Proc. of the Topical Meeting on Multidimensional Data Analysis, CERN (1976).
[31]P. Lornet, in: Proc. of the Topical Meeting on Multidimensional Data Analysis, CERN (1976).
[32]N. Manton, in: Proc. of the Topical Meeting on Multidimensional Data Analysis, CERN (1976).
[33]W. L. Koontz and K. Fukunaga, IEEE Trans. Comput. **C2**, 967 (1972).
[34]W. Jahn and H. Vahle, Die Faktorenanalyse und ihre Anwendung, Berlin (1970).
[35]H. Böttcher *et al.*, Nucl. Phys. **B81**, 365 (1974).
[36]M. Aderholz *et al.*, Nucl. Phys. **B8**, 45 (1968).
[37]J. Beaupré *et al.*, Nucl. Phys. **B46**, 1 (1972).
[38]H. Böttcher *et al.*, Preprint Zeuthen-PHE 76-7, Berlin (1976).
[39]H. Grässler *et al.*, Nucl. Phys. **B121**, 189 (1977).
[40]W. D. Nowak and H. Schiller, Preprint Zeuthen-PHE 75-12, Berlin (1975).
[41]R. Honecker *et al.*, Preprint CERN/EP/PHYS 77-51 (1977).
[42]C. N. Yang, Private communication.
[43]M. Korkea-aho, Preprint 75/88, Helsinki University (1975).
[44]P. Nyborg, Textbook in Elementary Particle Physics, Vollebekk (1972).
[45]R. Honecker *et al.*, Nucl. Phys. **B50**, 157 (1972).
[46]H. Grässler *et al.*, Nucl. Phys. **B113**, 365 (1976).
[47]M. Deutschmann *et al.*, Nucl. Phys. **B99**, 397 (1975).
[48]G. Otter *et al.*, Nucl. Phys. **B80**, 1 (1974).
[49]R. Honecker *et al.*, Nucl. Phys. **B106**, 365 (1976).
[50]A. Eskreys, in: Proc. of the Sixth Intern. Colloquium on Multiparticle Reactions, RL 75-143 (1975), p. 241.
[51]R. Harris, Preprint VTL-PUB-22, Washington University (1975).
[52]V. Chaloupka *et al.*, Phys. Lett. **B50**, 1 (1974).
[53]Th. Naumann and H. Schiller, in: Proc. of the Third Topical Meeting on Multidimensional Analysis, Nijmegen (1978), p. 54.
[54]P. M. Dauber *et al.*, Phys. Rev. **153**, 1403 (1967).
[55]E. Colton *et al.*, Nucl. Phys. **B17**, 117 (1970).
[56]Amsterdam-CERN-Nijmegen Collaboration, in: Proc. of the Fifth Intern. Symposium on Many Particle Hadrodynamics, Leipzig (1974).
[57]M. Deutschmann *et al.*, Nucl. Phys. **B36**, 373 (1972).
[58]W. Lohmann and H. J. Schreiber, Private communication.
[59]N. Schmitz, in: Proc. of the 1965 Easter School for Physicists, CERN (1965).
[60]M. Aguilar-Benitez *et al.*, Phys. Rev. **D6**, 29 (1972).
[61]C. Michael, Daresbury Lectures, 14, DL/R36 (1975).
[62]L. Becker and H. Schiller, Preprint Zeuthen-PHE 76-23.
[63]E. Byckling and K. Kajantie, Particle Kinematics, New York (1973), p. 202.

Translated by Julian B. Barbour